CONVENTION ON LONG-RANGE TRANSBOUNDARY AIR POLLUTION

UN/ECE INTERNATIONAL CO-OPERATIVE PROGRAMME ON EFFECTS ON MATERIALS, INCLUDING HISTORIC AND CULTURAL MONUMENTS

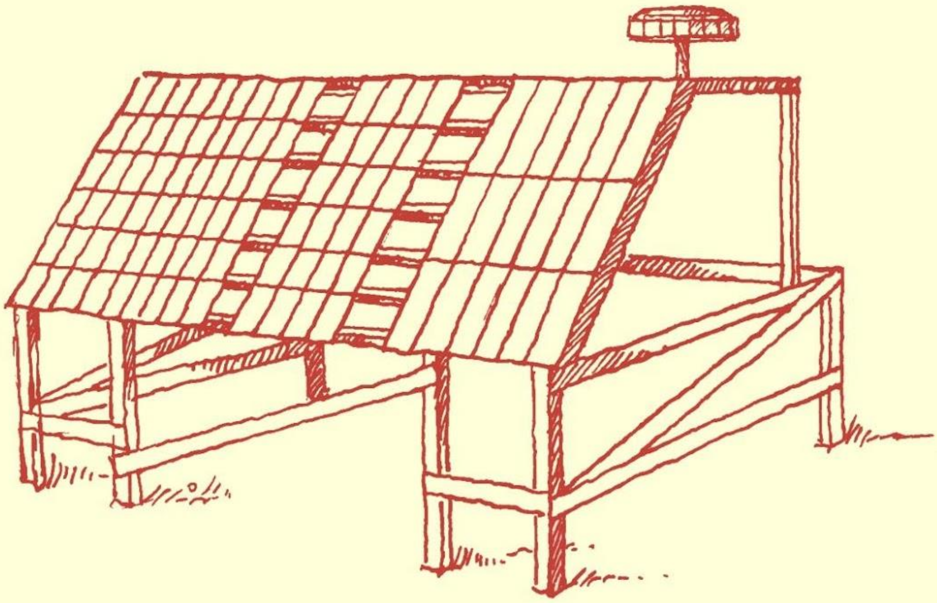

Report No 93:

Call for Data "Inventory and condition of stock of materials at UNESCO world cultural heritage sites". Part VI – The relationship between the environment and the artefact

September 2022

PREPARED BY THE SUB-CENTRE FOR STOCK OF MATERIALS AT RISK AND CULTURAL HERITAGE

Italian National Agency for New Technologies, Energy and Sustainable Economic Development (ENEA), Bologna, Italy

CONVENTION ON LONG-RANGE TRANSBOUNDARY AIR POLLUTION

**INTERNATIONAL CO-OPERATIVE PROGRAMME
ON EFFECTS ON MATERIALS,
INCLUDING HISTORIC AND CULTURAL MONUMENTS
(ICP Materials)**

Report No 93

Call for Data
"Inventory and condition of stock of materials at UNESCO world cultural heritage sites"

Part VI – The relationship between the environment and the artefact

Teresa La Torretta, Pasquale Spezzano

…

ENEA, Bologna, Italy
September 2022

http://www.enea.it/

CONTENTS

1 Introduction

The International Co-operative Programme on Effects on Materials, including Historic and Cultural Monuments (ICP Materials) was launched in 1985 within the scope and the activities of the Convention on Long-range Transboundary Air Pollution. The aim of the Programme is to fill some of the major gaps in scientific knowledge in the area of materials corrosion influenced by atmospheric pollutants by performing a quantitative evaluation of multi-pollutant effects on atmospheric corrosion on both technically important materials and materials used in historic and cultural monuments.

Many of the materials used in the construction of historic and cultural monuments are very sensitive to air pollution, resulting in corrosion and soiling of the materials which were used to create the artefacts. The Programme, through the Sub-Centre for stock of materials at risk and cultural heritage, agreed to launch a Call for Data on "Inventory and condition of stock of materials at UNESCO world cultural heritage sites". UNESCO sites are considered of outstanding universal value and are therefore ideal for illustration and dissemination of effects of air pollution on materials. The Call was approved at the 1st joint session of the Steering Body to the EMEP and the Working Group on Effects (Geneva, 14-18th September 2015) and then launched in October 2015.

Six Parties to the Convention, Croatia, Germany, Italy, Norway, Sweden and Switzerland, provided qualitative and quantitative data on both historic/cultural monuments and on concentrations of main air pollutants and meteo-climatic parameters measured at monitoring stations close to the selected UNESCO world cultural heritage sites. Taken together, the twenty-one cultural heritage objects included in the call have a total external surface area of about 430,000 m^2 and cover a wide range of materials (natural stone, artificial stone, copper, bronze, glass and others) as well as a wide range of environmental conditions. Detailed information on monuments/sites and their selection can be found in the ICP Materials Report No 80: Call for Data "Inventory and condition of stock of materials at UNESCO World Cultural Heritage sites", 2015-2017. Status Report" released in September 2017 (ICP Materials, 2017).
In the report ICP Materials Report No 83: "Call for Data-Inventory and condition of stock of materials at UNESCO World Cultural Heritage sites, Part II – Risk assessment" released in September 2018 (ICP Materials, 2018), the damage due to air pollution on the materials of these twenty-one cultural objects was assessed by using dose-response functions established by ICP Materials. In the subsequent report ICP Materials Report No 86: "Call for Data-Inventory and condition of stock of materials at UNESCO World Cultural Heritage sites, Part III – Economic evaluation" (ICP Materials, 2019) an assessment of the cost of damage due to corrosion and soiling from air pollution for the twenty-one unique monuments was reported on the basis of a well-recognized methodology for cost assessment developed in the EU REACH Project. The Report No 89 presented the assessment of the relative importance of individual pollutants and the effect of their reduction on the cost of pollution to some materials constituting the selected twenty-one objects of cultural heritage and a case study on the impact on the cost of damage on the Italian sites included in this study by using the forecasts of the national model MINNI (4x4km) on atmospheric concentrations of pollutants in 2030 following the measures that will be taken in Italy in response to the requests of the National Emission Ceilings Directive (EC, 2016) for reducing emissions. The last ICP Materials Report No. 90 reported the application of air quality models with increased resolution at selected UNESCO sites in Campania (Italy) to assess the damage on materials due to air pollution. EMEP MSC-W models (previous EMEP50 with resolution of 50x50Km, and actual EMEP01 with resolution 01°x01°) and Italian national model AMS-MINNI (resolution of 4x4km and 1x1Km) were considered.

Because of every monument is not an isolated entity this report "Part VI – The relationship between the environment and the artefact" concerns the study of the relationship between the environmental context surrounding some selected UNESCO sites and the air pollution responsible for the corrosion and soiling effects of the material.

On the basis of the economic evaluation reported in the report No.86 three UNESCO sites with different cost of maintaining due to air pollution were chosen: Saint Domnius, Split in Croatia, Wurzburg Residence, Bavaria, Germany and Royal Palace, Caserta, Italy.

2 Saint Domnius, Split, Croatia.

2.1 Geographic and climate profile of Split

The Republic of Croatia became an independent state on 8th October 1991. It is a member of the United Nations since 22nd May 1992 and of the European Union since 1st July 2013.

Fig.1- Croatia map and zoom on Split-Dalmatia[1]

Split-Dalmatia County borders on the north with the Republic of Bosnia and Herzegovina, on the west with Šibenik-Knin County and on the east with Dubrovnik-Neretva County (Fig.1). Split is the largest town of the region of Dalmatian and the second largest city of Croatia. It lies at the center of the eastern Adriatic coast on a peninsula between the eastern part of the Gulf of Kaštela and the Split Channel. The Marjan hill (178 meters), rises in the western part of the peninsula. The Kozjak (779 meters) and Mosor (1339 meters) ridges protect the city from the north and northeast, and separate it from the hinterland. (Wikipedia.org)

The geographic coordinates of Split are: 43°30′36″N 16°27′00″E.

The climate of Split is classified as Mild Mediterranean.
Summers are long, hot, sunny and moderately dry. Split receives more than 2,600 sunshine hours annually. Afternoons are characterized by the Mistral, a light and nice breeze. July is the hottest and the driest month with an average temperature around 28°C and total precipitation usually below 28 mm.
Winters are mild, wet and windy because of the strong cold northern wind Bura and the humid eastern-southern wind Jugo. Temperature rarely goes under 0°C and snow is extremely rare.
January is the coldest month, with an average temperature around 7 °C.
Autumn begins late and is wet: November is the wettest month, with a precipitation total of nearly 110 mm and 12 rainy days. (Državni hidrometeorološki zavod)
Because of its mild climate, Split is a popular tourist destination of the Adriatic Sea all over the year.

Table1- Air temperature and Precipitation averages for Split (https://meteo.hr/)

	Jan	Feb	Mar	Apr	May	Jun	Jul	Aug	Sep	Oct	Nov	Dec
AIR TEMPERATURE												
Mean [°C]	7.9	8.4	10.8	14.4	19.1	23.2	26.1	25.8	21.6	17.1	12.7	9.3
PRECIPITATION												
Total Prec. [mm]	77.9	66.2	63.3	62.6	57.3	50.1	27.6	38.6	71.6	78.8	113.4	103.3

[1] TUBS, CC BY-SA 3.0 via Wikimedia Commons

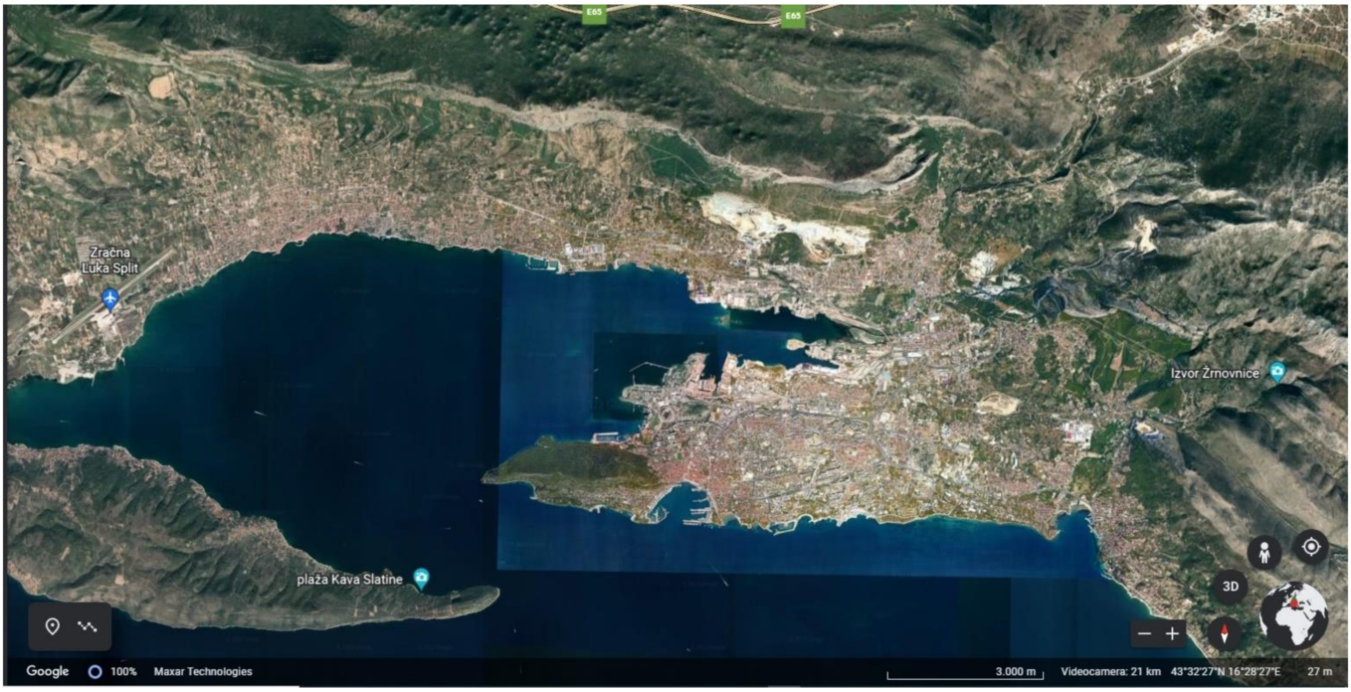

Figure 2 - The Split Urban Area[2]

2.2 Population

According to the Census performed by the Croatian Statistical Office (POPIS '21), in 2021 the total population of Croatia is 3,888,529, while the total population of Split-Dalmatia County is 425,412 inhabitants. The city of Split has 161,312 inhabitants with a population density of 2,032/km^2. In the table the settlements included in the administrative area of the City are reported.

Table 2 - Administrative area of Split settlements (POPIS'21)

		Ukupan broj stanovnika *Total population*
Split		161.312
	Donje Sitno	290
	Gornje Sitno	358
	Kamen	1.942
	Slatine	932
	Split	150.410
	Srinjine	1.205
	Stobreč	2.875
	Žrnovnica	3.300

[2]Google Earth Pro-Image Landsat/Copernicus

2.3 Energy

Figure 3 reports a simplified energy balance of Croatia (PROSPECT 2030)

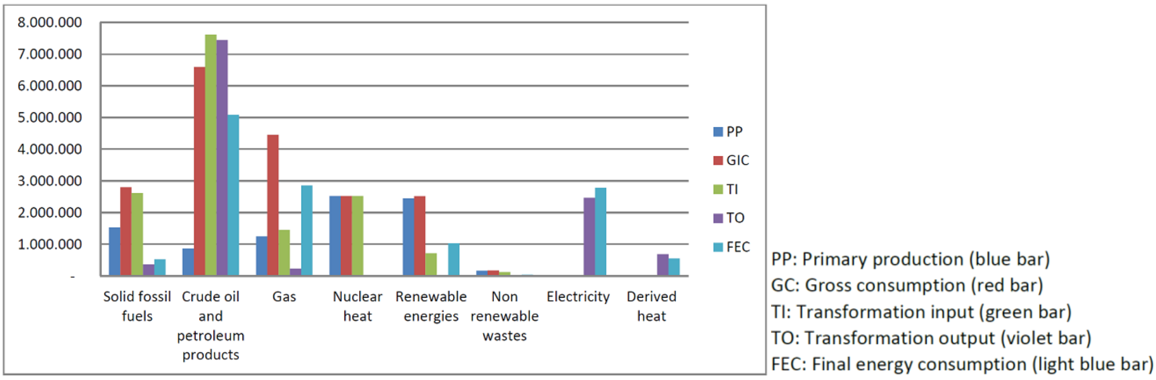

Figure 3 - Croatian simplified energy balance (PROSPECT 2030)

Because of the richness in water, in Croatia the production of electricity is characterized by use of hydro plant system (55% of total electricity production) that causes dependence on energy imports. In 2015 primary energy generation underwent a reduction of 6.7% compared to the previous year: adverse hydrology caused a consistent reduction of hydro power utilization. (Republic of Croatia-Ministry of Environment and Energy.
Croatian data energy consumption can summarize as follows: 84% Non-Industry, 15% Manufacturing Industry, 0.2% Extractive Industry and 0.7% Non- specified (Industry) (European Emission Agency).

In 2016 total demand of energy for Split-Dalmatian county was assessed at about 5,607 GWh, 7% of the total national consumption.
Crude oil and petroleum, followed by electricity are the most used fuel (Figure 4a). Renewable energies cover the 11% of requirement and they are used largely by residential sector for heating aims by means wood burning (Figure 5)
Transport sector presents the largest demand of energy (52%), followed by residential sector (24%), while the percentage attributable to industry sector is only 7% (Figure. 4b)

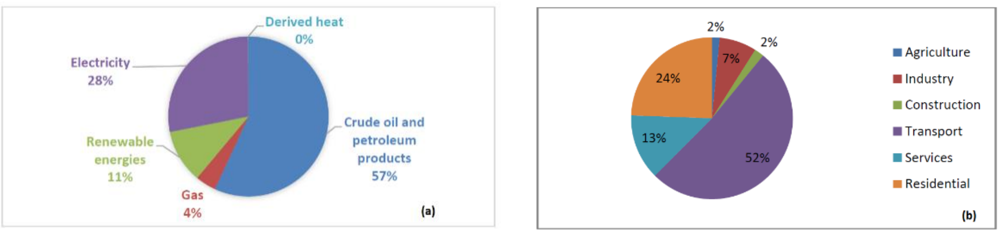

Figure 4 - Final energy consumption estimation for Split-Dalmatia County
by fuel (a) and by sector (b) 2016 (Prospect2030 -source: Croatian Bureau of Statistics])

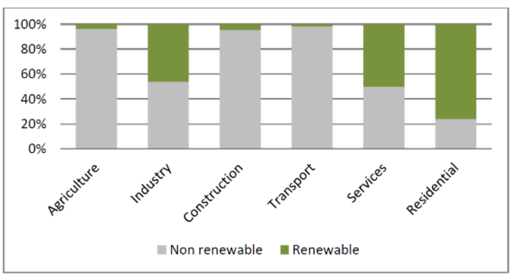

Figure 5 - Distribution of renewable energies for sector (Prospect2030)

As reported by the following table, electricity is produced only by renewable sources: 80% from hydro, 18% from wind and 2% from solar photovoltaic plants.

Table3 - Energy generation in Split-Dalmatia County (Prospect2030)

Electricity generation	*Installed capacity (MW_{el})*		*Energy generated (MWh per year)*	*Number of facilities*
Source	*Electricity only*	*Combined heat-power*	*Electricity*	
Hydro	919	-	2.426.000	5
Wind	226	-	545.500	8
Solar photovoltaic	30	-	42.326	24
Total	**1.176**	**-**	**3.013.826**	**37**
thereof non renewable	-	-	-	-
thereof renewable	*1.176*	-	*3.013.826*	*37*

As already mentioned, it could be a reduction of production of electricity by hydro, due to the inherent characteristics connected to hydrology.

2.4 Industry

According to the EUROSTAT data (EUROSTAT) the contribution to national GDP by Split-Dalmatia County is about 8.4%. In the following figures are reported the GDP per capita trend from 2015 to 2019. The values for Split-Dalmatia County are lower than for Croatia, but they present the same increasing trend.

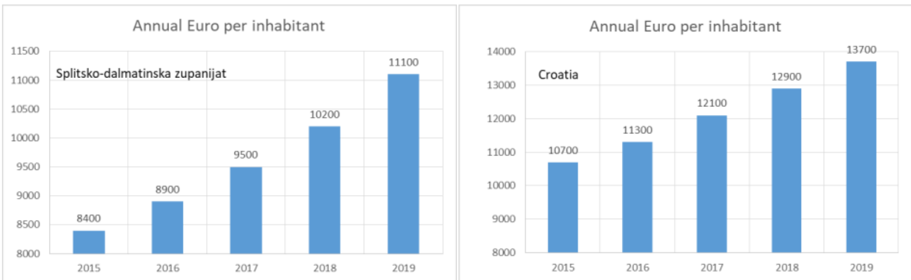

Figure 6 - GDP per capita trend for Croatia and Split-Dalmatia County; time range 2015-2019 (own elaboration from EUROSTAT data)

In the following figures national and local gross value added (GVA) per sector are reported on the base of EUROSTAT data

(a)

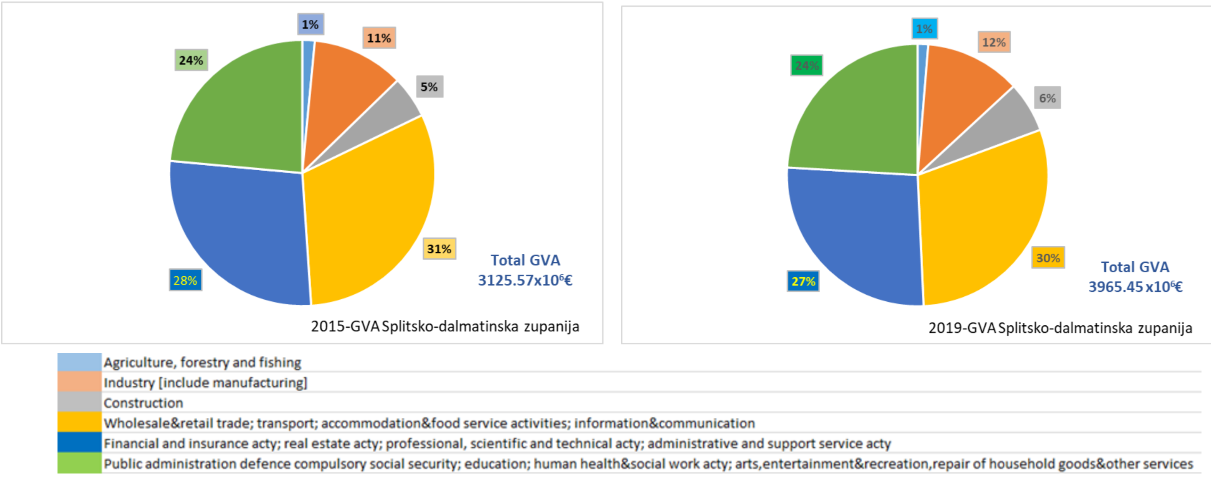

(b)

Figure 7 - annual national (a) and local (b) GVA-%. Years 2015 and 2019
(own elaboration from EUROSTAT data)

Regional wholesale and retail trade, transportation, accommodation and food service activities are larger than national ones, while industry sector is less present (food-fishing, olive, wine production, paper, concrete and chemicals) (Wikipedia). It is due to the strong tourist vocation of Dalmatia, moreover confirmed by the consistent contribute to regional GVA of real estate activities.

The Split-Dalmatia County has about 9% of the total national employees (EUROSTAT), the most part employed in the service sectors (figure 8).

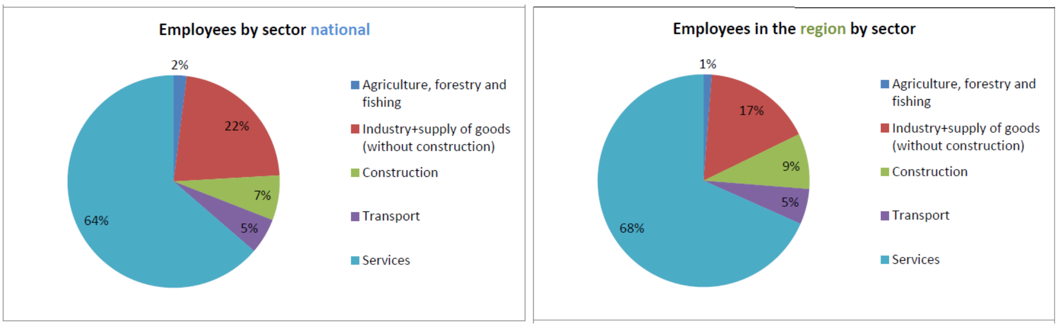

Figure 8 – National and local employees by sector (Prospect2030)

In Split-Dalmatia County the average annual registered unemployment rate decreased from 17% in 2017 to 14.3% in 2018, a little more than national data (12.1% in 2017 to 9.7% in 2018), but the average monthly net earnings are below the national average for ~12.1% (Croatian Bureau of Statistics)
To be mentioned Brodosplit the largest shipyard in Croatia. It employs around 2,300 people. (Wikipedia)

2.5 Transports and infrastructures

Relate to public transportation all parts of Split are connected by a network of buses (Official website of City of Split)

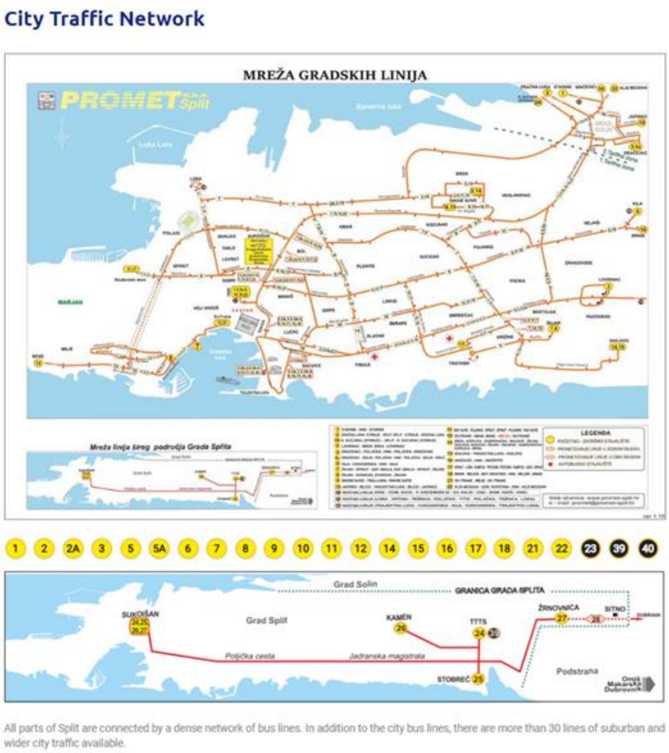

Figure 9 - Split public traffic network (Promet Split)

In Split-Dalmatia county rail transport is not the most used public transport. Split is connected with some municipalities as Primorski Dolac and the Town of Kaštel, and through the counties of Šibenik-Knin and Zadar is connected to Zagreb (HŽ INFRASTRUKTURA-https://eng.hzinfra.hr).

Figure 10 - Railway system in Split-Dalmatia County (HŽ INFRASTRUKTURA)

Usually bus transport is preferred to rail transport for saving time. At passenger service more than 30 lines are available for suburban and wider city traffic.

Figure 11 - Suburban public traffic network (Promet Split)

122 km of motorways, 770 km of state roads and 1,749 km of county and local roads are the numbers of road network in Split-Dalmatia County that is the biggest road network in Croatia. (www.wikipedia.en)
The A1 motorway (Zagreb-Split-Dubrovnik) is the longest Croatian motorway, 476.3 kilometers, and it has played an important role on trade and tourism activities improvement

Split Airport, located in Kastela, is the second busiest airport in terms of passenger traffic in the Republic of Croatia, 3,301,930 in 2019 (http://www.split-airport.hr), with national and some European connections that increase during the summer months .

Two seaports are in Split: passengers-ferry port on the south and the commercial port (for loading/unloading of general cargo, storage of various cargo and loading/unloading of freight from railway wagons) on the north of the peninsula.
As it is possible to read on the Split Port site (www.portsplit.hr/en): "Since its establishment, the Port of Split has been continuously investing in port infrastructure, with the aim of providing excellent conditions and services in passenger traffic, as well as increasing the competitiveness of its cargo port and freight traffic.
The natural position and size of the port of Split enabled its rapid development and it became a port of special – international economic interest for the Republic of Croatia.
Also, thanks to its strategic position in the Mediterranean (between Venice and the Aegean port), the port of Split is one of the most important ports of call for cruises in the Adriatic, and its long history and numerous sights attract thousands of tourists."

In the table is reported the traffic in port of Split during 2017 (Ladislav Stazić et al.,2020)

Table 4- Marine traffic in Port of Split during 2017 (Ladislav Stazić et al.,2020)

Ship type	Number of vessels
Cruise	232
Bulk Carrier	330
Tanker	115
Container	40
General/other	57
Total	**774**

From the HEIP (Energetski Institut HRVOJE POŽAR) data (https://eihp.hr/en/?lang=en) in Split-Dalmatia county 224,818 are the registered stock of motor vehicles in 2017, about the 10.8% of national vehicles, summarized for type of vehicles as in table 5.

Table 5 - National and local distribution by type of motor vehicles

Motor vehicles by type	Regional	National
Passenger cars	177418	1605013
Motorcycles	26399	156334
Lorries	16873	155636
Buses	687	5683
Road tractors	1333	16497
Other motor vehicles	2108	130362
Total	224818	2069525

Petrol and diesel are most used fuel by passenger's cars (Figure 12).

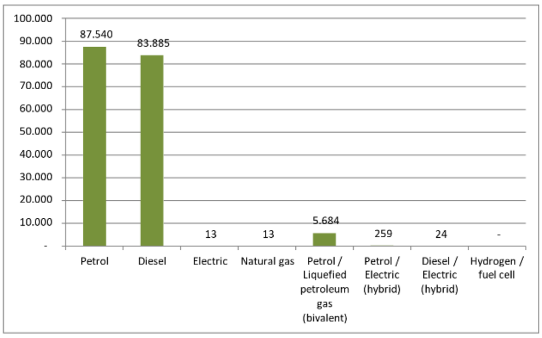

Figure 12 - Cars by fuel in Split-Dalmatia county [source: EIHP 2017]

2.6 Emission inventories

Spatially distributed emission data as used in EMEP models were downloaded by EMEP Centre on Emission Inventories and Projections (CEIP).
The resolution of grid emissions is 0.1°x0.1° long-lat.
Geographic coordinates of Saint Domnius Cathedral in Split match to cell 16.45; 43.55 of the grid.
In this report were considered emissions into air of following main pollutants:
NO_x, SO_x, NH_3, NMVOC, CO and PM_{10}.
Sectors are defined as GNFR source category (UNECE 2015, Guidelines CE/EB.AIR/128.UNECE)
Aviation sector isn't considered because no airport is included in the concerned cell of the grid.
Public Power isn't considered because it isn't reported by Croatian inventory.
The next tables 6 and 7 include total emission contribution in Mg/year per sector.
Figures 13 and 14 report the contribution of each pollutant for each sector in percentage to the total annual emissions.

Table 6 - Sector contribution (Mg) to the annual total emissions for Split. Year 2015 (Data source: EMEP/CEIP 2021)

Year 2015	NOx	SOx	NH3	NMVOC	CO	PM10	Total
	Mg	Mg	Mg	Mg	Mg	Mg	Mg
Industry	1644.85	33.16	0.65	58.72	2551.91	251.17	**4540.45**
OtherStationaryComb	39.83	8.07	10.82	86.54	665.81	100.95	**912.02**
Fugitive				26.63			**26.63**
Solvents	0.61	0.12	1.37	409.51	18.52	13.61	**443.75**
RoadTransport	337.61	0.44	6.73	127.97	686.71	22.37	**1181.83**
Shipping	135.73	0.02	0.01	4.84	12.79	2.59	**155.99**
Offroad	61.52	0.04	0.02	14.60	192.52	3.01	**271.70**
Waste	0.08		0.83	0.00		6.01	**6.92**
AgriLivestock	3.26	0.00	3.71	2.82		0.65	**10.44**
AgriOthe			9.36	1.02	0.05	1.46	**11.89**
Total	**2223.48**	**41.85**	**33.50**	**732.66**	**4128.31**	**401.83**	**7561.62**

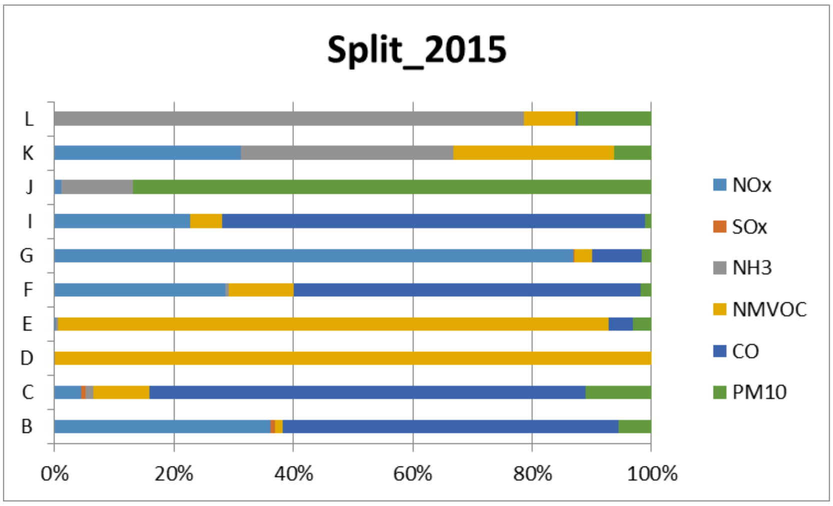

L	AgriOthe
K	AgriLivestock
J	Waste
I	Offroad
G	Shipping
F	RoadTransport
E	Solvents
D	Fugitive
C	OtherStationaryComb
B	Industry

Figure 13 - Sector contribution (%) to the annual total emissions for Split. Year 2015 (Data source: EMEP/CEIP 2021)

Table 7 - Sector contribution (Mg) to the annual total emissions for Split-year 2019 (Data source: EMEP/CEIP 2021)

Year 2019	NOx	SOx	NH3	NMVOC	CO	PM10	Total
	Mg	Mg	Mg	Mg	Mg	Mg	**Mg**
Industry	940.11	26.56	0.69	55.79	2150.07	239.70	**3412.91**
OtherStationaryComb	35.45	4.70	9.11	74.11	564.68	81.71	**769.76**
Fugitive				23.81			**23.81**
Solvents	0.88	0.21	1.99	713.14	26.92	20.51	**763.66**
RoadTransport	341.78	0.00	5.40	89.98	490.27	19.95	**947.39**
Shipping	161.75	0.03	0.01	5.77	15.25	3.09	**185.90**
Offroad	48.51	0.04	0.02	10.93	165.45	2.11	**227.07**
Waste			0.81	0.00		6.39	**7.20**
AgriLivestock	0.07		3.14	2.36		0.54	**6.12**
AgriOthe	3.62	0.00	10.69	1.03	0.06	1.43	**16.83**
Total	1532.18	31.54	31.87	976.94	3412.69	375.43	**6360.65**

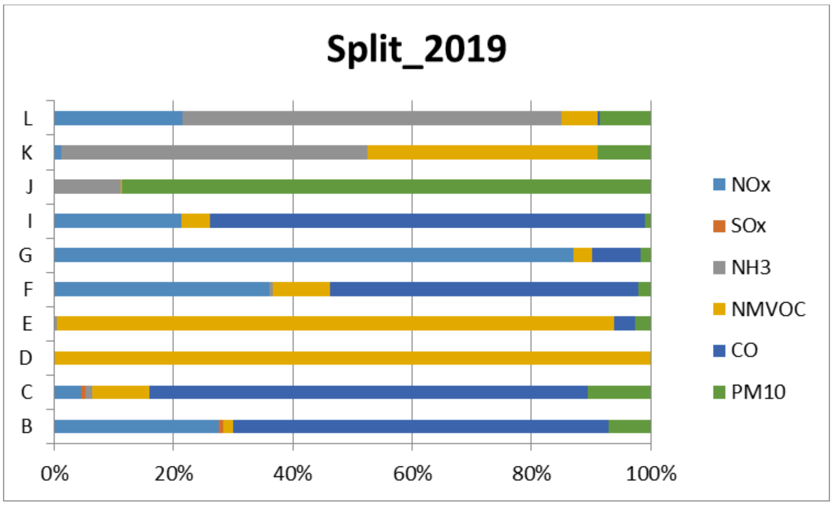

L	AgriOthe
K	AgriLivestock
J	Waste
I	Offroad
G	Shipping
F	RoadTransport
E	Solvents
D	Fugitive
C	OtherStationaryComb
B	Industry

Figure 14 - Sector contribution (%) to the annual total emissions for Split. Year 2019 (Data source: EMEP/CEIP 2021)

In terms of sectors the highest contribution is ascribed to Industry followed by Road transport and Other Stationary Combustion. Industry appears to hold the majority of CO and NO_x emissions. Comparing 2015 and 2019, emissions due to Solvents and Shipping sectors have increased. Development of port activity in the last years has risen with an important increase in traffic. A study published by Croatian researchers remarks the contribution to total emissions of Split port activities according to type of ships, comparing emissions coming from cargo and passenger traffic, highlighting that cruise ships activity contributes consistently to the amount of emissions (Ladislav Stazić et al., 2020).

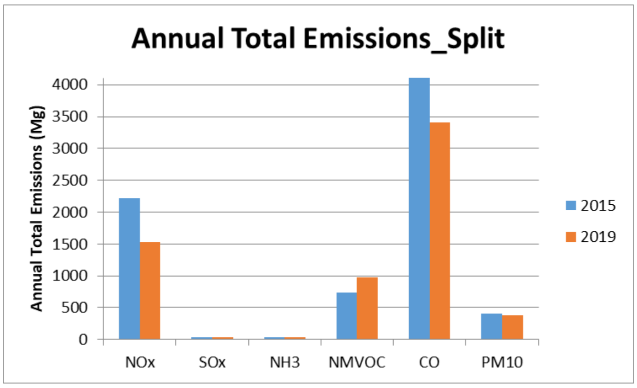

Figure 15 - Annual total emissions of main pollutants into air in Split. Comparison 2015 and 2019 (Data source: EMEP/CEIP 2021)

In Figure 15 the contribution of each pollutant to the total annual emission is reported as a comparison between years 2015 and 2019.
A general light decrease of emissions in air is evident during the considered time range except for NMVOC connected for the most part to Solvents sector.
In terms of pollutants CO and NO_x emissions, both connected for the most part to Industry and Road transport sectors, show the highest values even if from 2015 their values have decreased more than the other ones.

2.7 Air Quality - Ground level air pollutants

Air pollutants monitoring stations	
Split_Split-1-traffic	43.510653; 16.449342
Castel Sucurac_AMS1-background	43.548119; 16.434961
Sveti Kajo_AMS2-background	43.545906; 16.467836

Figure 16 - Position of air pollutants monitoring stations in Split[3]

The air pollutants data in Split were downloaded by official site Kvaliteta zraka u Republici Hrvatskoj collected by the local network of monitoring stations (Figure 16): Split-1 as traffic station, AMS-1 as urban background, and AMS2 as suburban background.
Split-1 is the closest monitoring station to Saint Domnius. Unfortunately Ozone concentration data are not available for these stations. Ozone average data measured in other two stations having similar geographic characteristics to Split (Opuzen and Podaca located North and South of Split) were used. In Figure 17 air pollutants data are reported for investigated range time: 2015-2019. To appreciate the trend over the past the data for the three stations concentration are reported after removing Ozone concentration values too.

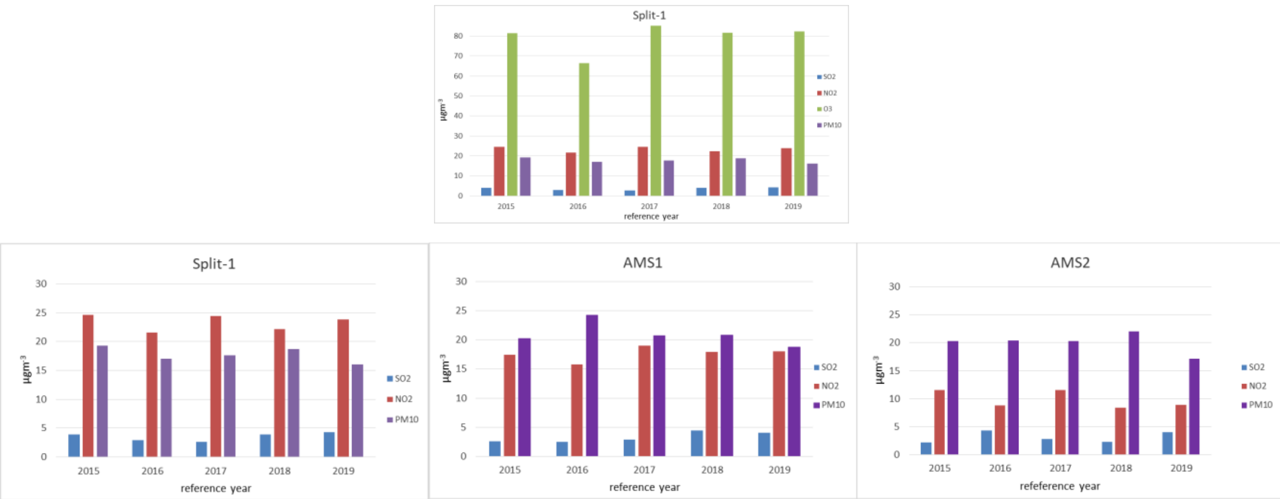

Figure 17 - Air pollutants data by monitoring station Split-1, AMS1 and AMS2. Time range: 2015-2019 (own elaboration from Kvaliteta zraka u Republici Hrvatskoj data)

[3] Google Earth Pro-Image Landsat/Copernicus

The UNESCO site Saint Domnius is closer to urban traffic monitoring station, Split-1.
The concentration values of NO_x decrease from more to less bustling areas: Split-1 shows the highest values of NO_x concentration.
PM_{10} concentration values are nearly the same for the three monitoring stations, it could be attributed to sea spray.
As expected, concentrations of SO_2 have dropped significantly and now do not represent an important air polluting compound: SO_2 concentrations are low and constant along the time.
NO_x and PM_{10} concentrations show a slight decrease in the considered temporal range.

2.8 Implications on the UNESCO Cultural Heritage Site: The Cathedral of Saint Domnius

Figure 18 - Aerial photo of Saint Domnius[4]

Even if Split was founded as the Greek colony of Aspálathos in the 3rd or 2nd century, Split history is strictly linked to the Diocletian's Palace. The Roman emperor around the year 305 retired close to Salona, where he was born, and built a summer residence of around 30,000 square meters, protected by strong external walls to fight barbarian invasions. Today Diocletian's palace is one of the most important and better preserved monuments of Ancient Rome. The Cathedral of Saint Domnius is an imperial mausoleum dating back to late Antiquity, located within Diocletian's Palace from which the medieval town of Split originated. It is part of a larger complex around the Peristyle where the Palace's north-south street (cardo) and the east-west oriented street (decumanus) meet, which was surrounded by other pagan temples. Diocletian's Palace and the medieval town of Split were inscribed on the UNESCO World Heritage List in 1979. Every year around 300,000 people visit the cathedral and the bell tower. An increasing number of tourists places a significant burden on the complex but also poses a threat and a risk to this World Heritage site.

The construction of Diocletian's mausoleum began at the end of the 3rd century within an enclosed area of temenos (sacral area) in the south-eastern part of the imperial palace. Octagonal structure was built using carved stone blocks, with a vaulted dome and bricks laid in a fish-scale pattern. The interior consists of a circular floor plan divided by rectangular and semicircular niches, and of two rows of granite columns, with intricate stone cornices and upper frieze with portraits of Diocletian and his wife Prisca and erotes, depicting hunting scenes. A crypt is located within the high base platform of the mausoleum. A peripter surrounds the complex and consists of marble and stone columns with the remains of stone panels. When converting the pagan mausoleum into a cathedral, a five-storey stone bell tower was constructed on the west side between the 13th and 16th centuries, while a deep chorus (choir area) was added to the eastern side at the beginning of the 17th century.

An extensive renovation of the cathedral was carried out at the end of the 19th century, when the

[4] Google Earth Pro-Image Landsat/Copernicus

dilapidated segments of stone sculpture were replaced in the interior of the building. The major restoration of the bell tower was completed in 1908. The roof of the mausoleum was renovated in 1996 and the static restoration of the chorus lasted from 1999 until 2002. When repairing the court located south of the cathedral, waters, damaging the floor of the former mausoleum, were also eliminated. Conservation and restoration works on the interior side of the dome and stone walls were carried out continuously from 2012 until 2015, and the restoration of the medieval floor tiling and the lower floor was carried out from 2016 until 2017, using the technique opus sectile.
The restoration works of the Cathedral's exterior have been carried out on the main portal and in the atrium at the bell tower base, which displayed noticeable level of damage and stone surface soiling such as salt sediment, calcification, black sediment, micro-discontinuity, corrosion and iron impurities in the stone. The atrium also houses marble bas-reliefs with inscriptions that required specific treatment. The interior has been darkened from centuries of burning candles, and parts of the stone sculptures have been affected by soluble salts, calcite deposits, black crusts and micro discontinuity.
The relatively small Cathedral is frequently visited by large tourist groups which is disadvantageous for the rich movable heritage housed (wooden doorways and pews dating from the 14th century, easel paintings, gilded wood, silver) as it may cause variations in humidity and temperatures. There is also a prominent abrasion of the stone stairways leading from the entrance to Peristyle.
The methodology of conservation - restoration works depended on the level of damage and results of laboratory testing on samples. The methodology applied includes: dust suction using a suction device, hand washing using sterilized water with a low concentration of solvent, extraction and stabilization of soluble salts, mechanical removal of calcite deposits using precise hand tools (scalpels and micro drills), extraction and replacement of corroded iron elements with new elements of stainless steel, laser cleaning, reconstruction of micro-discontinuity in stone, use of artificial stone in cementing smaller defects (stone dust, acrylic-lime mortar) with finishing treatments using traditional tools, filling flash (spew) lines with lime mortar, stone surface protection using suitable chemical agents for consolidation and impregnation.
Fragments of medieval headstones have been cleaned in the same manner, they were joined together with micro rods made of stainless steel and missing elements were reconstructed. The floor in opus sectile technique was cleaned with neutral agents, lined and consolidated, and then documented and protected with geotextile.

St. Domnius Cathedral is located in the center of Split between seaside and bustling area. NO_x emissions are mainly due to the traffic and the industrial activity. However, even if NO_x emissions due to port activities are lower than the previous ones, they show an increasing trend connected to the increasing port traffic.
The high number of sunshine hours can influence photochemical pollution.

Nitric acid is not measured by the Split Air Quality Monitoring Network, so atmospheric nitric acid concentrations were calculated from NO_2, O_3, relative humidity (Rh) and temperature (T) by using the following empirical function derived within the MULTI-ASSESS project (MULTI- ASSESS, 2005):

$$\mathbf{HNO_3 = 516 \times e^{-3400/(T+273)} ([NO_2] \times [O_3] \times Rh)^{0.5}}$$

where

$[HNO_3]$ = annual average concentration, µg m^{-3}
$[NO_2]$ = concentration, µg m^{-3} - annual average
$[O_3]$ = concentration, µg m^{-3} - annual average

T = temperature, °C – annual average
Rh = relative humidity, % - annual average

The methodology used for the estimation of the damage due to attack of atmospheric pollutants at the selected UNESCO cultural heritage sites is based on the use of the dose-response functions, first year exposure, for the multi-pollutant situation:

$$\mathbf{R = 4.0 + 0.0059[SO_2]Rh_{60} + 0.054Rain[H^+] + 0.078[HNO_3]Rh_{60} + 0.0258PM_{10}}$$

where

R = surface recession, µm
Rh_{60} = Rh – 60 when Rh > 60, 0 otherwise (Rh = relative humidity, % - annual average)
Rain = amount of precipitation, mm year^{-1} - annual average
$[SO_2]$ = concentration, µg m^{-3} - annual average
$[H^+]$ = concentration, mg l^{-1} - annual average
$[HNO_3]$ = annual average concentration, µg m^{-3}
PM_{10} = annual average concentration, µg m^{-3}

The multi-pollutant dose-response function relates damage to limestone, expressed as surface recession rate, to a range of atmospheric pollutants: sulphur dioxide (SO_2), nitric acid (HNO_3), total acidity of rainfall (H^+), and particulate matter (PM_{10}). Environmental parameters also play a role, as reflected by the presence in the dose-response function of the two terms amount of precipitation (Rain) and relative humidity (Rh).

Figure 19 shows the corrosion graphs for limestone based on the pollution data for the city of Split related to the year 2015-2019. Between 2015 and 2019 it is possible to observe a slight decrease of the recession rate for limestone.

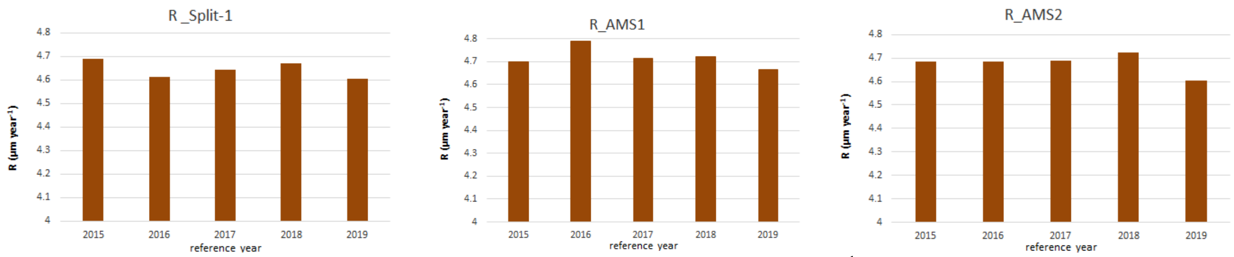

Figure 19 - Surface recession, µmyear^{-1}

Predicted soiling rate of limestone in Split was calculated by applying the dose- response function:

$$\mathbf{\Delta R/Ro = 1 – exp(-PM_{10} \times t \times K)}$$

Where
ΔR/Ro = relative loss of reflectance,
PM_{10} = concentration of PM_{10} (µg m^{-3}),
t = time (days),
K= soiling constant.

For limestone a soiling constant of 6.5 x 10^{-6} could be used, but it isn't officially accepted because of

its high variability. So to be conservative the same calculation has been made using the lowest soiling constant reported on Mapping Manual, 3.47 x 10^{-6} for Polycarbonate Membrane material. In this way it is possible to assert with a good approximation that the value of **Δ**R/Ro is within the calculated range.
This dose-response function was used to predict the years to reach 30% of loss in reflectance as a function of the ambient PM_{10} concentrations to which the material is exposed.
30% of loss in reflectance is the "tolerable soiling before action", which represents the threshold triggering significant adverse public reaction of what constitutes acceptable soiling (Mapping Manual Ch.4).
In the following figures the number of years for reaching 30% of loss in reflectance on the basis of PM_{10} measured by the three monitoring stations in Split is reported.

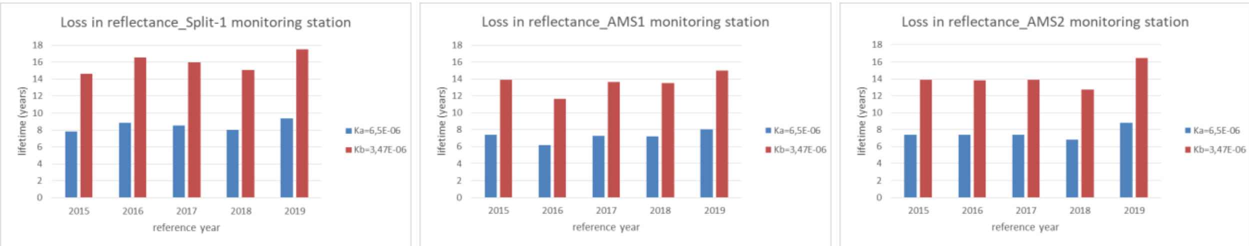

Figure 20 - Estimated lifetime of limestone for soiling (30% of loss in reflectance)

For cultural heritage objects a period of 10-15 years between cleaning operations is considered to be appropriate.
Considering the lowest value for the constant, the 2050 target of 15 years is reached. On the other hand, considering the highest constant value, lifetime increases but far from the 2050 target.

2.9 References

Census of Population, Households and Dwellings in the Republic of Croatia- Popis21-Državni zavod za statistiku 2021- https://popis2021.hr/popisni-upitnik-engleski.html

City of Split: Official website https://www.split.hr/

Croatian Bureau of Statistics. Persons in Paid Employment, by Activities and Counties - Situation as on March 2018.

DHMZ -Državni hidrometeorološki zavod- https://meteo.hr

EMEP Centre on Emission Inventories and Projections (CEIP) https://www.ceip.at/the-emep-grid/gridded-emissions

European Emission Agency https://www.eea.europa.eu/themes/industry/industrial-pollution/industrial-pollution-country-profiles)

EUROSTAT, Population change - at regional level (NUTS3). Eurostat metadata 2019. https://ec.europa.eu/eurostat/cache/metadata/en/demo_r_gind3_esms.htm

HEIP - Energetski Institut HRVOJE POŽAR - https://eihp.hr/en/?lang=en

HŽ INFRASTRUKTURA https://eng.hzinfra.hr

Ladislav Stazić, Radoslav Radonja, Vladimir Pelić, Branko Lalić "The Port of Split international marine traffic emissions inventory" *Journal of Maritime Research* 34 (2020) 32-39 © https://doi.org/10.31217

Mapping manual Ch.4 https://www.umweltbundesamt.de/en/document/mapping-manual-ch-4

MULTI-ASSESS, 2005. MULTI-ASSESS. Model for multi-pollutant impact and assessment of threshold levels for cultural heritage. Final report. http://www.corr-institute.se/MULTI-ASSESS/

Nele Veldeman, Wim van der Maas Spatial mapping of emissions EMEP/EEA air pollutant emission inventory guidebook 2019 - https://www.eea.europa.eu/publications/emep-eea-guidebook-2019/part-a-general-guidance-chapters/7-spatial-mapping-of-emissions

Prospect2030- Interegg Central Europe-2019 Deliverable D.T2.2.5- Split and Dalmatia Energy Report Version n°0.1/2019 https://www.interreg-central.eu/Content.Node/PROSPECT2030.html

Republic of Croatia- Ministry of Environment and Energy_7th national Communication and 3rd biennial report of the Republic of Croatia under UNFCCC (2018)

Promet Split https://www.promet-split.hr/

Split Airport website: http://www.split-airport.hr

Split Port website: www.portsplit.hr/en

UNECE 2015, Guidelines for Reporting Emissions and Projections Data under the Convention on Long-range Transboundary Air Pollution. ECE/EB.AIR/128.

3 The Residence, Würzburg, Bavaria, Germany.

3.1 Geographic and climate profile of Würzburg

The city Würzburg is not part of the homonym district, although it is completely enclosed by it. It is located in the Lower Franconia Region, in the north of the German State of Bavaria.

Fig. 21 – Germany and Bayern maps

Figure 22 - Aerial photo of Würzburg[5]

It is crossed by the Main River and located between Frankfurt am Main and Nurnberg.
Würzburg covers an area of 87.6 square kilometers and lies at an altitude of around 177 meters.

The geographic coordinates of Würzburg are: 49°47′40″ N 9°55′46″E

The climate of Würzburg is classified as Humid Temperate. The annual average temperature is around 9.4°C. Over the year temperature varies from around -2°C and 24°C.
Summers are comfortable and partly cloudy and go on from June to the beginning of September. July

[5] Google Earth Pro-Image Landsat/Copernicus

is the hottest month with an average high temperature of about 24°C and low of about 14°C.
The cold season goes on from the half of November to the beginning of March, with an average daily high temperature below 7°C. The coldest month of the year in Würzburg is January, with an average low of -2°C and high of 3°C.
Precipitations are poor (an annual average of between 600-700 mm). The period with most wet days is between the months May and June, while February is the driest. Usually snow falls during the cold season. (https://weatherspark.com/)

Table 8. Air temperature and precipitation averages for Würzburg

	Jan	Feb	Mar	Apr	May	Jun	Jul	Aug	Sep	Oct	Nov	Dec
AIR TEMPERATURE												
Mean (°C)	1	1	5	9	14	17	19	19	15	10	5	2
PRECIPITATION												
Total Prec. (mm)	64	53	63	53	72	67	69	59	59	61	66	73

3.2 Population

Population of Würzburg, at 31 December 2020, was 126,954 inhabitants, while population density per km^2 is about 1449 inhabitants per km^2 on a total territory of 87.6 km² (Bayerisches Landesamt für Statistik).
The oldest Bavarian University, Julius-Maximilians-Universität, has a high student population, more than 30,000 students.
It is the administrative seat of the Regierungsbezirk Lower Franconia.

3.3 Energy

Despite most of the electricity generated in the lower Franconia comes from renewable sources, the electrical energy that was consumed in Würzburg in 2016 came primarily from the local conventional power plants. Photovoltaics is the most common technology with around 55% of the installed renewable energy capacity contributing for about 30 percent of the total power generation (Fig). (source: Jacqueline Escher, M. *Energieatlas 2018* Sc. Geographie Industrie- und Handelskammer Würzburg-Schweinfurt K.d.ö.R.)

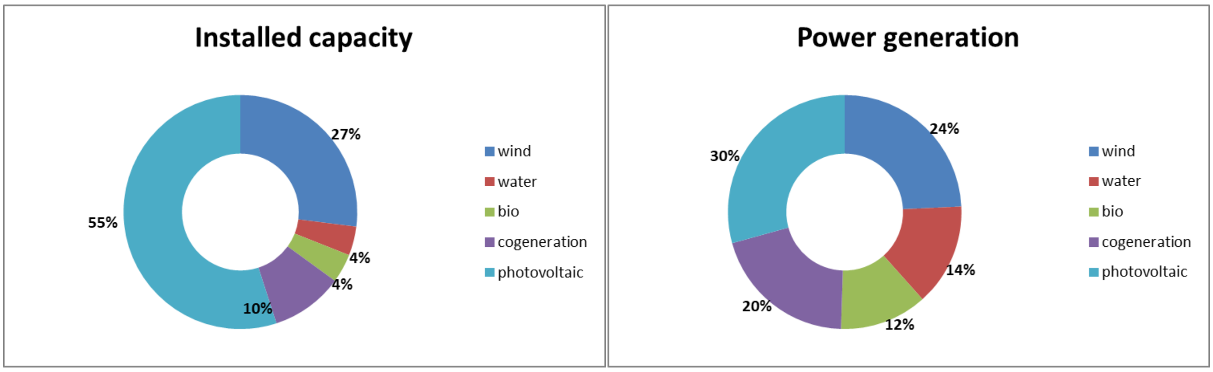

Figure 23 - Installed capacity and contribution to power generation by renewable energy sources (data from Energieatlas)

Energy sources such as hydropower or biomass make a strong contribution to total electricity generation around 25 %, despite relatively low installed capacity.

From 2012 to 2016, the energy transition also progressed in Mainfranken. Renewable energies with an output of almost 660 megawatts were added.
Accordingly, power generation has also increased in the region. In particular, the generation of electricity from photovoltaic and wind power has risen sharply due to the construction of new plants. With the introduction of the so-called 10H regulation in Bavaria, new expansion of wind power plants has been decreased. On the other hand, the generation of electricity by the regional conventional power plants has declined slightly.

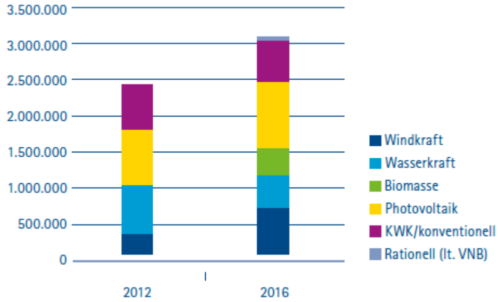

Figure 24 - Power generation in Mainfranken in 2012 and 2016 by energy source (MWh/a) (Source: Energieatlas)

The region of Lower Franconia cannot cover its electricity needs from its own generation. Electricity consumption in 2016 was 5,213 gigawatt hours (GWh) compared to the generation of 3,429 GWh – this corresponds to around 65 percent of consumption (Figure 8). Electricity consumption itself has hardly changed since 2012. Savings through energy efficiency technologies will increasingly be compensated for by more and different consumers in the electricity sector - such as electromobility or increased digitization. The region is therefore still dependent on electricity imports from other (neighboring) regions.

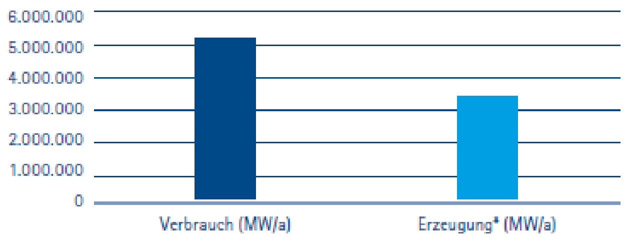

Figure 25 - Power consumption (Verbrauch) and Power generation (Erzeungung) in Mainfranken 2016 (Source: Energieatlas)

High electricity consumption is mainly due to a high proportion of manufacturing industry or a high population density: the city Würzburg is the most populous city in the region with a corresponding concentration of trade and services.

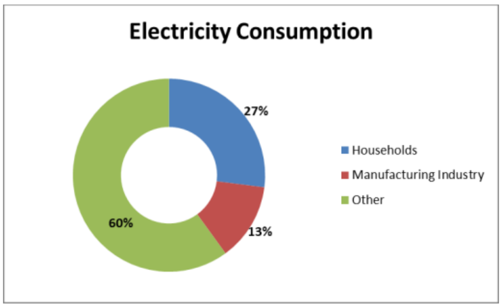

Figure 26 - Electricity consumption in the city of Würzburg (data from Energiealtlas)

In Figure 26 Electricity consumption in the city of Würzburg is reported shared between households, manufacturing and others, whereby the term "other" mainly includes trade and services, but also street lighting. Almost two thirds of the electricity consumption in the city of Würzburg is accounted for by this area. A large part of the consumption is likely to be caused by the healthcare sector. Würzburg as the administrative center should not be underestimated in terms of electricity consumption.

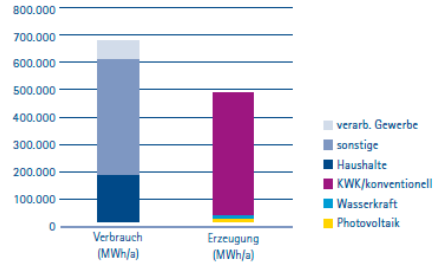

Figure 27 - Comparison of electricity consumption (Verbrauch) and generation (Erzeugung) in the city of Würzburg, 2016

The electrical energy that was consumed in Würzburg in 2016 came primarily from the local conventional power plants. Renewable sources, on the other hand, play a subordinate role. Just less than five percent of the electricity is generated from renewable sources using hydroelectric power and photovoltaics. Hydropower as a base load capable renewable energy source contributes around 1.2 percent.

3.4 Industry

According to the EUROSTAT data the contribution to regional GDP by Würzburg is about 15.5%. In the following figures are reported the GDP per capita trend from 2015 to 2019. The values for Würzburg are larger than for Unterfranken Region. (Reference Eurostat).

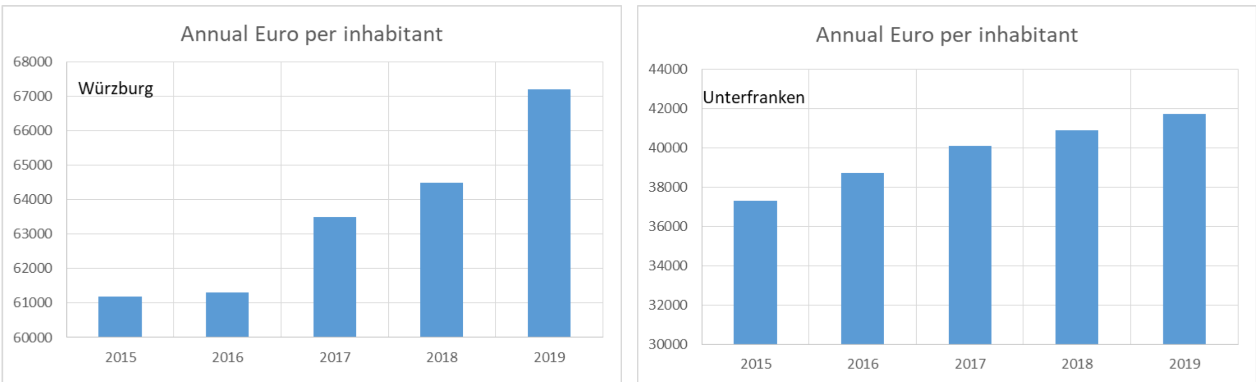

Figure 28 - GDP per capita trend for Würzburg and Unterfranken; time range 2015-2019 (from Eurostat data)

In the following figures regional and local gross value added (GVA) per sector are reported.

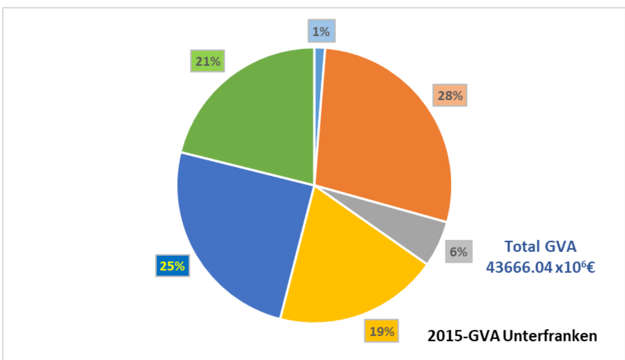

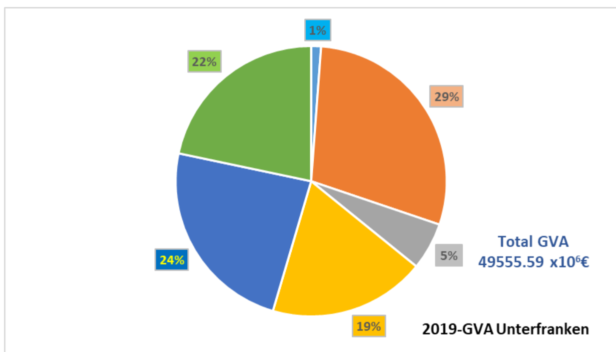

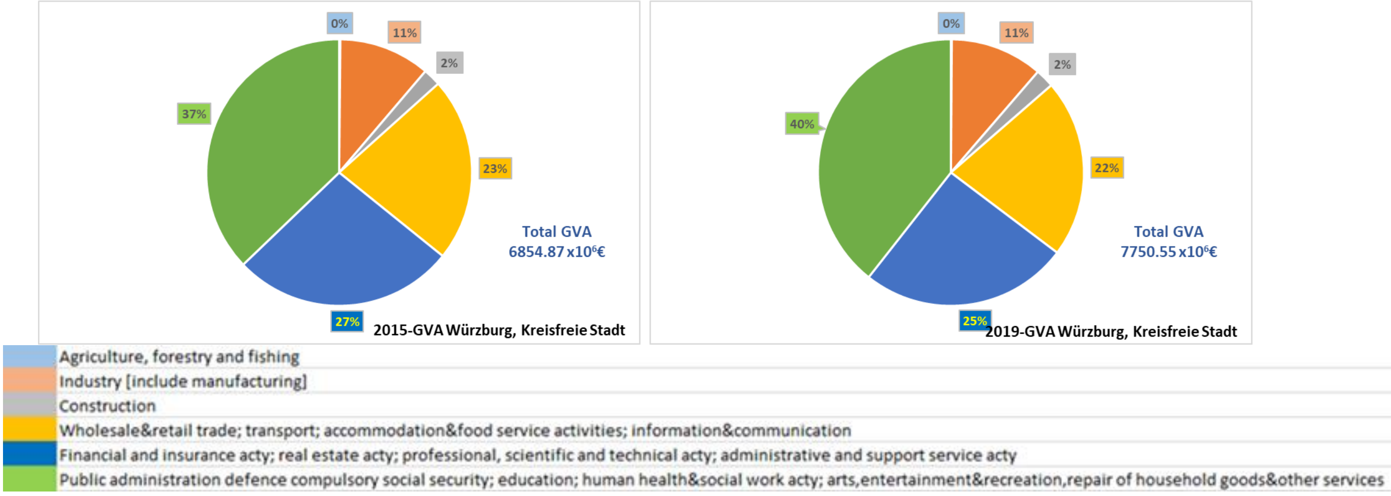

Figure 29 - Annual national and local GVA-%. Years 2015 and 2019 (EUROSTAT data)

Compared with Unterfranken Region it is evident the importance assumed for the economy of Würzburg especially by some sectors such as education, scientific and technical activities. The Julius-Maximilians-University is the oldest Bavarian university, founded in 1402 in Bavaria, with more than 30,000 students providing "a continuous stream of thinkers and doers. In addition, Würzburg as an education site offers a thorough portfolio of recognized training programs for trade, industry and commerce" (https://www.wuerzburg.de/en).

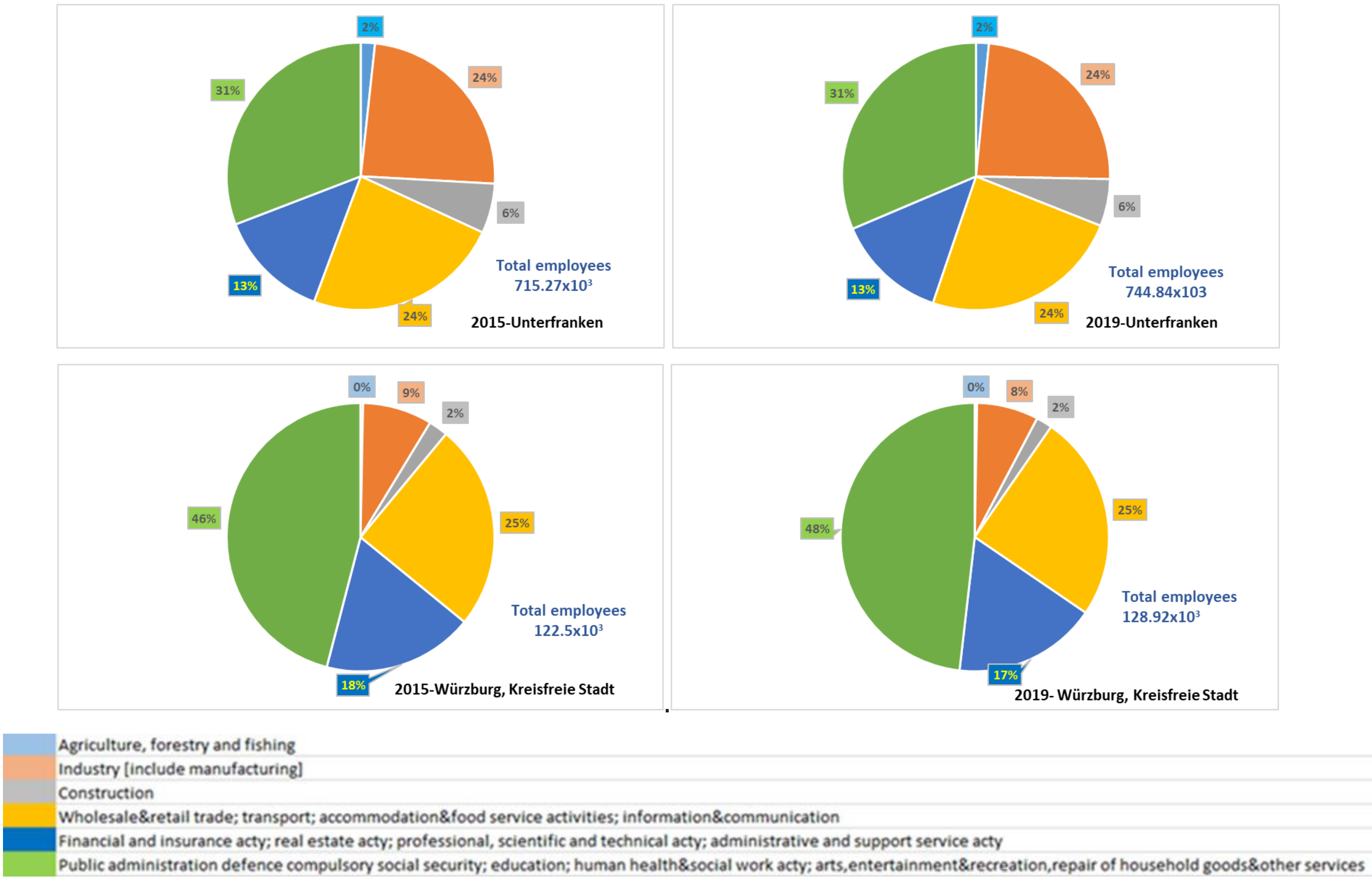

Fig 30 - Total employed person per sector in Unterfranken and in Wurzburg. Years 2015 and 2019 (own elaboration from Eurostat data)

The largest employees are in administrative sectors, especially at Julius-Maximilians-University and the municipality. The tertiary sector is the most substantial with over 80% of the workforce (Energieatlas)

In the Private sector Fahrzeugteile (mechatronic) and Koenig & Bauer (printing machines) are the industries with the largest number of employees.

Würzburg is known as the capital of the German wine region Franconia which is famous for its mineral-rich dry white wines, especially from the Silvaner grape. Würzburger Hofbräu brewery also locally produces a well-known pilsner beer.

A curiosity: Würzburg is home to the oldest pizzeria in Germany. Nick di Camillo opened his restaurant named *Bier und Speisewirtschaft Capri* on 24 March 1952.

3.5 Transport and infrastructure

The German Federal Government recently, in May 2022, ratified a plan to encourage the use of public transportation by offering a monthly public transit pass for a stunning price of just nine euro from 1th June 2022 to 31th August 2022. With "Das 9 Euro Fahrticket" it can travel as many times as they want across all forms of public transport throughout Germany, including buses, U-Bahns, S-Bahns, trams, and local and regional trains for one calendar month. Useful initiative to reduce using private vehicles.

Public transportation in Wurzburg is managed by VVM Gmbh (https://www.vvm-info.de/)

Figure 31-VVM lines in Wurzburg by aerial photo (VVM)

Public transport network consists of buses and trams. Following the schemes of bus and tram lines with a focus on the tram network.

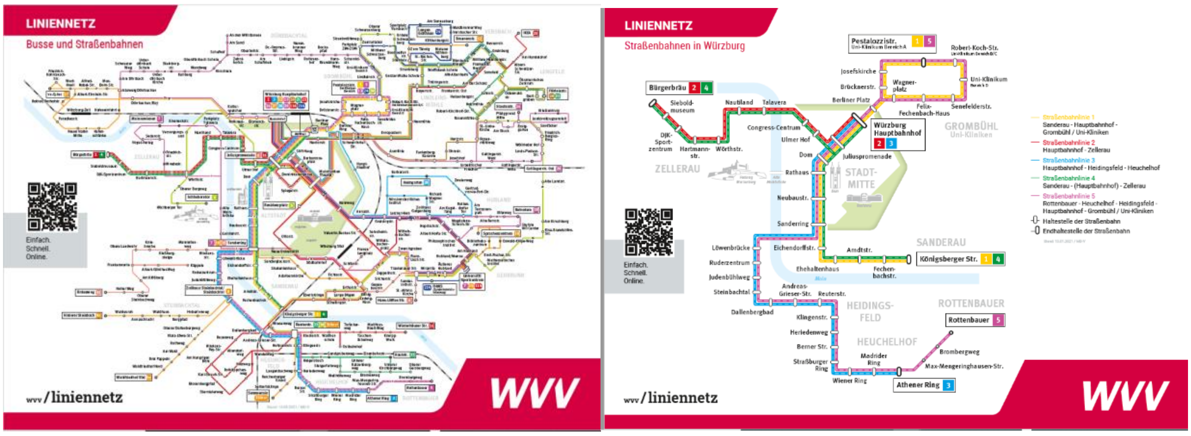

Figure 32 - Bus and tram lines in Wurzburg (VVM)

VVM offers a good public transport during the night too, as it is possible from the following night network-map

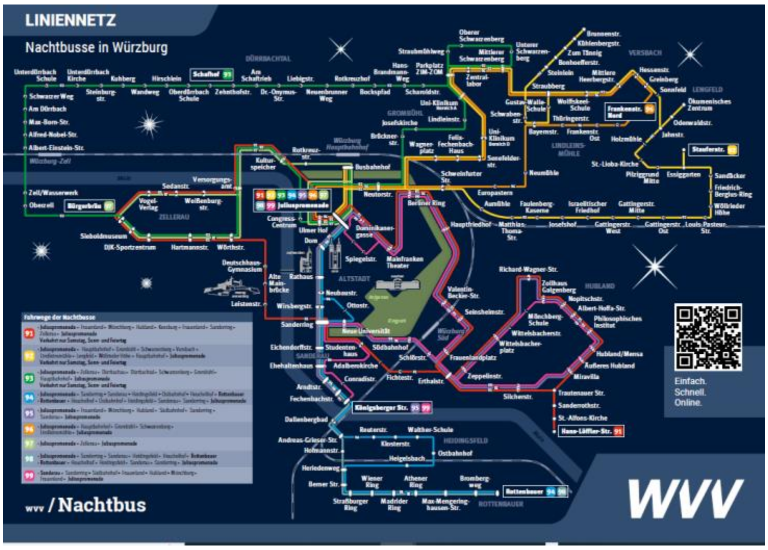

Figure 33 - Wurzburg bus lines: night network-map (VVM)

VVM website is interactive: all information you need about the city (and the district too), is located with the way to reach it.
A lot of bicycle lanes are located throughout the city and the Main-Radweg long-distance bicycle trail passes through the old town.
Wurzburg is well-connected by railway with all the main German towns and three international airports plus a regional district airport are located within a radius of 150 km.
The river Main connects Würzburg to the European network of waterways – equally important for the transport of bulk goods and river cruise tourists.
"In a linked transport system, public transport has been organized in exemplary fashion not only in the city but also in the whole district."(https://www.wuerzburg.de/)
Interchange of three of the most important federal freeways, A 3, A 7 and A 81 pass through the city of Würzburg

3.6 Emission inventory

Spatially distributed emission data as used in EMEP models were downloaded by EMEP Centre on Emission Inventories and Projections (CEIP).
The resolution of grid emissions is 0.1°x0.1° long-lat.
Geographic coordinates of Würzburg Residence in Würzburg match to cell 9.95; 49.75 of the grid.
In this report were considered emissions into air of following main pollutants:
NO_x, SO_x, NH_3, NMVOC, CO and PM_{10}.

Sectors are defined as GNFR source category (UNECE 2015, Guidelines CE/EB.AIR/128.UNECE).

Aviation sector isn't considered because no airport is included in the concerned cell of the grid.

The next tables include total emission contribution in Mg/year per sector
Figures 34 and 35 report the contribution of each pollutant for each sector in percentage of the total annual emissions.

Table 9 – Sector contribution (Mg) to the annual total emissions for Würzburg- year 2015 (Data source: EMEP/CEIP 2021)

Year 2015	NOx	SOx	NH3	NMVOC	CO	PM10	Total
	Mg	Mg	Mg	Mg	Mg	Mg	Mg
PublicPower	215.38	46.88	1.04	12.39	100.79	4.63	**381.11**
Industry	164.74	28.24	7.82	44.04	152.71	55.40	**452.95**
OtherStationaryComb	129.58	21.14	2.64	70.79	959.97	41.00	**1225.13**
Fugitive	0.55			24.46			**25.02**
Solvents	0.38	0.21	1.06	541.44	22.98	8.39	**574.47**
RoadTransport	564.69	0.82	8.87	113.23	1128.42	33.34	**1849.37**
Shipping	26.50	0.55	0.01	1.19	4.14	1.03	**33.41**
Offroad	47.03	0.13	0.02	20.74	262.46	5.60	**335.99**
Waste	0.32	0.07	3.72	21.39	20.31	6.62	**52.42**
AgriLivestock	0.45		67.97	60.67		2.84	**131.92**
AgriOthe	13.43		36.55	1.25		2.59	**53.82**
Total	**1163.05**	**98.05**	**129.68**	**911.59**	**2651.78**	**161.44**	**5115.59**

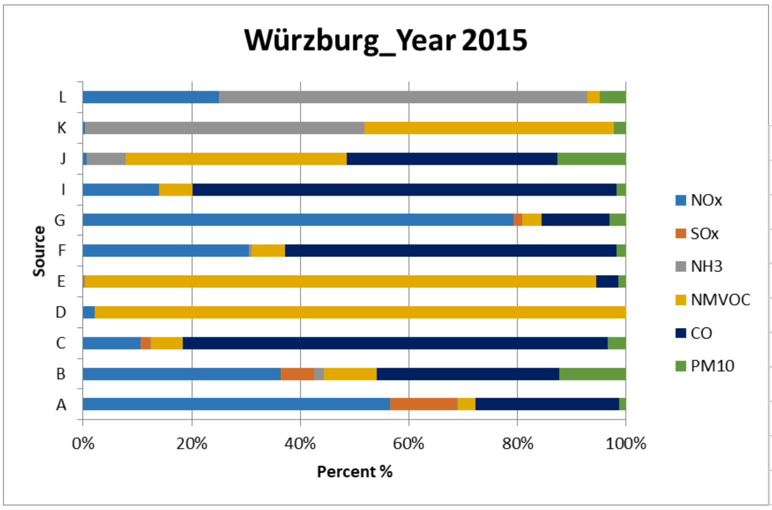

L	AgriOthe
K	AgriLivestock
J	Waste
I	Offroad
G	Shipping
F	RoadTransport
E	Solvents
D	Fugitive
C	OtherStationaryComb
B	Industry
A	PublicPower

Figure 34 – Sector contribution (%) to the annual total emissions for Würzburg. Year 2015 (Data source: EMEP/CEIP 2021)

Table 10 – Sector contribution (Mg) to the annual total emissions for Würzburg- year 2019 Data source: EMEP/CEIP 2021)

Year 2019	NOx	SOx	NH3	NMVOC	CO	PM10	Total
	Mg	Mg	Mg	Mg	Mg	Mg	Mg
PublicPower	81.97	19.28	0.88	9.47	80.48	2.95	**195.04**
Industry	158.18	24.68	7.13	45.06	126.38	57.02	**418.46**
OtherStationaryComb	128.38	12.22	2.62	67.41	799.90	35.62	**1046.14**
Fugitive				24.87			**24.87**
Solvents	0.35	0.19	1.00	553.93	21.57	7.62	**584.66**
RoadTransport	423.26	0.83	8.02	103.12	1005.83	30.45	**1571.51**
Shipping	24.60	0.60	0.01	1.13	3.59	1.03	**30.95**
Offroad	39.59	0.13	0.02	18.43	245.78	4.95	**308.90**
Waste	0.29	0.06	3.53	18.99	18.50	6.29	**47.65**
AgriLivestock	0.43		64.12	58.21		2.67	**125.42**
AgriOthe	11.78		32.14	1.08		2.55	**47.55**
Total	**868.82**	**58.02**	**119.47**	**901.69**	**2302.01**	**151.14**	**4401.17**

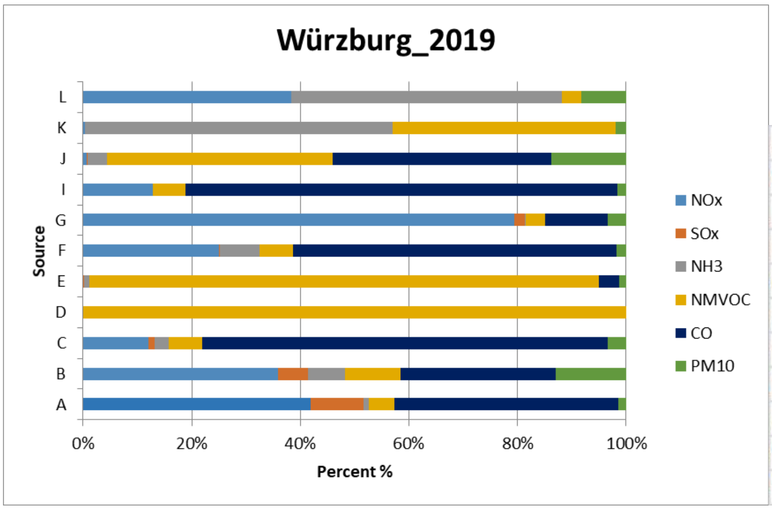

L	AgriOthe
K	AgriLivestock
J	Waste
I	Offroad
G	Shipping
F	RoadTransport
E	Solvents
D	Fugitive
C	OtherStationaryComb
B	Industry
A	PublicPower

Figure 34 – Sector contribution (%) to the annual total emissions for Würzburg. Year 2015 Data source: EMEP/CEIP 2021)

In terms of sectors the highest contribution is ascribed to Road Transport followed by Other Stationary Combustion and Solvents as expected on the basis of economy in Würzburg mainly connected to administrative, education and service economical activities.
Road Transport appears to hold the majority of CO and NO_x emissions.
Except Solvents all sectors show a decreasing trend into the concerned temporal range.

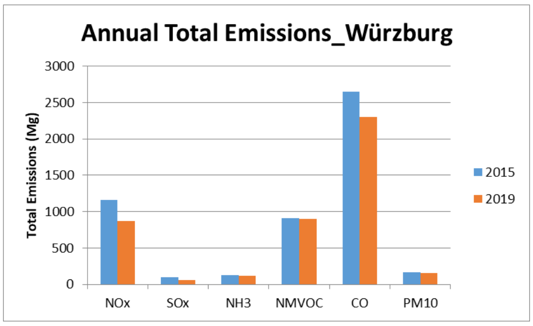

Figure 35 - Annual total emissions of main pollutants into air in Würzburg. Comparison 2015 and 2019

In Figure 35 the contribution of each pollutant to the total annual emission is reported as a comparison between years 2015 and 2019.
All emissions show a decreasing trend or nearly constant values as for NMVOC connected for the most part to Solvents sector.

3.7 Air Quality - Ground level air pollutants

Air pollutants monitoring stations	
Würzburg_Standtring Sud urban traffic	49.7946; 9.9359
Würzburg_Kopfklinic suburban background	49.8047; 9.9564

Figure 37: Position of air pollutants monitoring stations in Wurzburg[6]

The air pollutants data in Würzburg were downloaded by Bavarian State Office for the Environment (Bayerisches Landesamt für Umwelt) collected by the local monitoring stations (Figure 37): Standtring Sud as urban traffic station, and Kopfklinic as suburban background.
Standtring Sud is the closest monitoring station to the Würzburg Residence. Unfortunately SO_2 concentration data are not measured by these two monitoring stations. SO_2 concentration data were downloaded by EMEP MSC-W model.
Ozone concentration data measured by Kopfklinic station can be considered valid for Standtring Sud monitoring station too.
In Figure 38 air pollutants data are reported for investigated temporal range: 2015-2019.

Figure 38 – Air pollutants data by monitoring station Standtring Sud and Kopfklinic. Time range 2015-2019 (own elaboration from Bayerisches Landesamt für Umwelt data and EEA)

[6] Google Earth Pro-Image Landsat/Copernicus

The UNESCO site Würzburg Residence is closer to urban traffic monitoring station, Standtring Sud. The concentration values of NO_x decrease from more to less bustling areas: Standtring Sud shows the highest values of NOx and PM_{10} concentration.
As expected concentrations of SO_2 have dropped significantly and now does not represent an important air polluting compound: SO_2 concentrations are low and constant along the time.
NO_x and PM_{10} concentrations show a decrease in the considered temporal range, higher for urban traffic station.

3.8 Implications on the UNESCO Cultural Heritage Site: The Würzburg Residence

Figure 39 - Garden facade of Würzburg Residence, Würzburg[7]

The Würzburg Residence (49°47′34″N/09°56′21″E), the splendid palace of the prince bishops, and one of the finest Baroque buildings in Bavarian, Germany, is located in the Residenzplatz in Würzburg. Formally, the residence is a building with several courtyards and a large Cour d'Honneur. The dimensions are enormous: the garden front is 169 m long, the narrow side 92.6 m. The building comprises more than 300 rooms.
Balthasar Neumann, court architect of the Bishop of Würzburg, was the principal architect of the Residence, which was commissioned by the Prince-Bishop of Würzburg Johann Philipp Franz von Schönborn and his brother Friedrich Carl von Schönborn in 1719, and completed in 1744. Giovanni Battista Tiepolo, a Venetian painter, drew frescoes in the building, assisted by his son Domenico.
The interior rooms are considered as masterworks of Baroque/Rococo or Neoclassical architecture and art, including the grand staircase, the chapel, and the Imperial Hall. The building was heavily damaged during World War II, and restoration has been in progress since 1945. Since 1981, the Residence has been a UNESCO World Heritage Site.
The facades of the Residence are built of sandstone (Werksandstein) while the socket is made of limestone (Quaderkalk). The masonry consists of brickwork.
History:
1720 - 1744 Construction of the building
1737 - 1781 Stucco-work decoration and paintings in the interior
1945 Destruction by bombing
1945 - 1987 Reconstruction of the building and its interiors

Nitric acid is not measured so atmospheric nitric acid concentrations were calculated from NO_2, O_3, relative humidity (Rh) and temperature (T) by using the following empirical function derived within the MULTI-ASSESS project (MULTI-ASSESS, 2005):

$$\mathbf{HNO_3 = 516 \times e^{-3400/(T+273)} ([NO_2] \times [O_3] \times Rh)^{0.5}}$$

where

$[HNO_3]$ = annual average concentration, µg m^{-3}
$[NO_2]$ = concentration, µg m^{-3} - annual average

[7] Image by Rainer Lippert, source: www. wikipedia.de

$[O_3]$ = concentration, μg m^{-3} - annual average
T = temperature, °C – annual average
Rh = relative humidity, % - annual average

The methodology used for the estimation of the damage due to attack of air pollutants at the selected UNESCO cultural heritage sites is based on the use of the dose-response functions, first year exposure, for the multi-pollutant situation:

$$\mathbf{R = 4.0 + 0.0059[SO_2]Rh_{60} + 0.054Rain[H^+] + 0.078[HNO_3]Rh_{60} + 0.0258PM_{10}}$$

where

R = surface recession, μm
Rh_{60} = Rh – 60 when Rh > 60, 0 otherwise (Rh = relative humidity, % - annual average)
Rain = amount of precipitation, mm $year^{-1}$ - annual average
$[SO_2]$ = concentration, μg m^{-3} - annual average
$[H^+]$ = concentration, mg l^{-1} - annual average
$[HNO_3]$ = annual average concentration, μg m^{-3}
PM_{10} = annual average concentration, μg m^{-3}

The multi-pollutant dose-response function relate damage to limestone, expressed in terms of rate of surface corrosion, to a range of atmospheric pollutants: sulphur dioxide (SO_2), nitric acid (HNO_3), acidity of rainfall (H^+), and particulate matter (PM_{10}). Environmental parameters also play a role, as reflected by the presence in the dose-response function of the two terms amount of precipitation (Rain) and relative humidity (Rh).

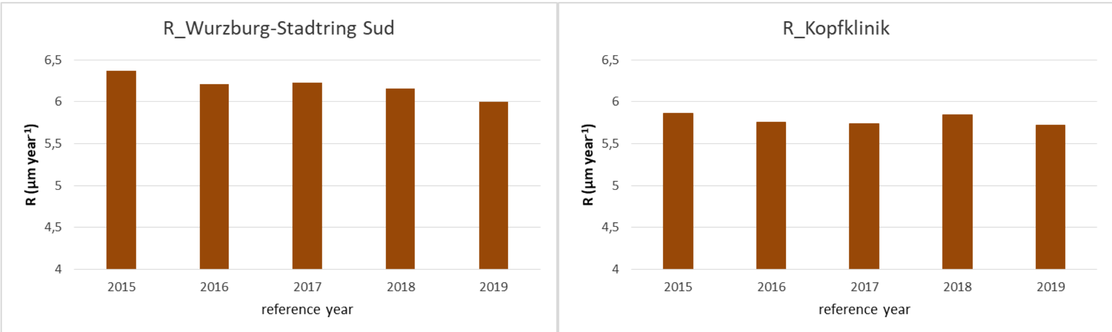

Figure 40 – Surface recession, μm$year^{-1}$

Figure 40 shows the corrosion values for limestone based on the pollution data for the city of Würzburg related to the year range 2015 – 2019. It is possible to observe a slight decrease of the recession rate for limestone more pronounced for urban traffic station.

Predicted soiling rate of limestone in Würzburg was calculated by applying the dose-response function:

$$\mathbf{\Delta R/Ro = 1 - exp(-PM_{10} \times t \times K)}$$

where
ΔR/Ro = relative loss of reflectance,

PM_{10} = concentration of PM_{10} ($\mu g\ m^{-3}$),
t = time (days)
K = soiling constant.

For limestone a soiling constant of 6.5×10^{-6} could be used, but it isn't officially accepted because of its high variability. So to be conservative the same calculation has been made using the lowest soiling constant reported on Mapping Manual, 3.47×10^{-6} for Polycarbonate Membrane material. In this way it is possible to assert with a good approximation that the value of $\Delta R/Ro$ is within the calculated range.
This dose-response function was used to predict the years to reach 30% of loss in reflectance as a function of the ambient PM_{10} concentrations to which the material is exposed.
30% of loss in reflectance is the "tolerable soiling before action", which represents the threshold triggering significant adverse public reaction of what constitutes acceptable soiling (Mapping Manual Ch.4).
In the following figures the number of years for reaching 30% of loss in reflectance on the basis of PM_{10} measured by the two monitoring stations in Würzburg is reported.

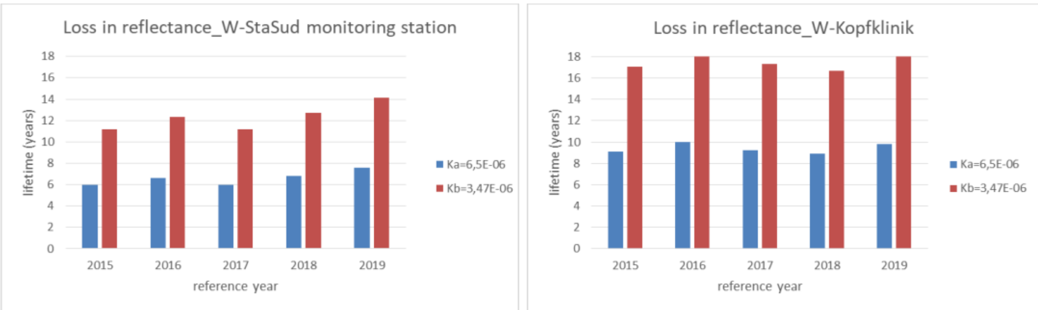

Figure 41 – Estimated lifetime of limestone for soiling (30% of loss in reflectance)

For cultural heritage objects a period of 10-15 years between cleaning operations is considered to be appropriate. Considering the lowest value for the constant the 2050 target of 15 years is reached, on contrary considering the highest constant value, loss of reflectance increases but far from the 2050 target.

3.9 References

Bayerisches Landesamt für Statistik https://www.statistikdaten.bayern.de /"Tabellenblatt "Daten 2", Statistischer Bericht A1200C 202041 Einwohnerzahlen der Gemeinden, Kreise und Regierungsbezirke". Bayerisches Landesamt für Statistik (in German). June 2021

Bayerisches Landesamt für Umwelt 2021 https://www.lfu.bayern.de/luft/immissionsmessungen/index.htm

EMEP Centre on Emission Inventories and Projections (CEIP) https://www.ceip.at/the-emep-grid/gridded-emissions

European Environment Agency- Data and Maps- Airbase, https://discomap.eea.europa.eu/App/AirQualityStatistics/index.html

EUROSTAT, 2015. Transport statistics at regional level. http://ec.europa.eu/eurostat/statistics-explained/index.php/

Mapping manual Ch.4 https://www.umweltbundesamt.de/en/document/mapping-manual-ch-4

MULTI-ASSESS, 2005. MULTI-ASSESS. Model for multi-pollutant impact and assessment of threshold levels for cultural heritage. Final report. http://www.corr-institute.se/MULTI-ASSESS/

UNECE 2015, Guidelines for Reporting Emissions and Projections Data under the Convention on Long-range Transboundary Air Pollution. ECE/EB.AIR/128.

VVM website https://netzplan.vvm-info.de/

Weatherspark https://weatherspark.com/

4 The Royal Palace of Caserta, Caserta, Italy

4.1 Geographic and climate profile of Caserta

Campania located in the southern part of Italy is the most populous and most densely populated region in the South. It is located between the Tyrrhenian Sea to the southwest and the southern Apennines to the northeast. The region borders to the north-west with Lazio, to the north with Molise, to the north-east with Puglia and to the east with Basilicata.

Figure 42 – Campania Region and aerial photo of Caserta[8]

Caserta is located on the edge of the Campanian plain at the foot of the Campanian Sub Apennine mountain range.
It is located 40 kilometers north of Naples.
From an urbanistic point of view Caserta is physically joined to neighboring towns without a break.

The geographic coordinates of Caserta are: 41°5' 3"12 N; 14°20' 8"88 E.

The climate of Caserta is classified between Mediterranean climate and a humid subtropical (muggy especially in the summer)
Caserta is located on the plain of Campania affected by the influences of the sea, especially during the winter with mild temperatures and higher humidity. Eventually cold periods don’t last long. It snows very rarely. Summers are very long, hot and sunny.
The driest month is July with total precipitation of 21 mm, while November is the wettest month, with a precipitation total of nearly 187 mm.
With an average temperature of 25° C August is the hottest month. The coldest month is January with an average temperature nearly 7°C.

Table 11 – Air temperature and precipitation averages for Caserta (climate-data)

	Jan	Feb	Mar	Apr	May	Jun	Jul	Aug	Sep	Oct	Nov	Dec
AIR TEMPERATURE												
Mean (°C)	7	7	10	13	17	22	24	25	20	16	12	8
PRECIPITATION												
Total Prec. (mm)	115	109	109	105	68	34	21	26	95	143	187	141

[8] Google Earth Pro-Image Landsat/Copernicus

4.2 Population

According to ISTAT on 1st January 2022 the total population of Italy was 58,983,122, the total population of Campania was 5,590,681 inhabitants. The city of Caserta had 73,068 inhabitants with a population density of about 1350/km^2.

4.3 Energy

The production and consumption of energy in Italy data source is by TERNA S.p.A., that "process the official statistics of the entire national electricity sector and are responsible for official communications to international bodies such as Eurostat, IEA, OECD, UN"
Trend of energy production by source for the time range between 2000 and 2020 is reported in Figure 43, while in Table 12 the amounts of energy production by source are reported for Campania and Caserta for the years 2015 and 2019.

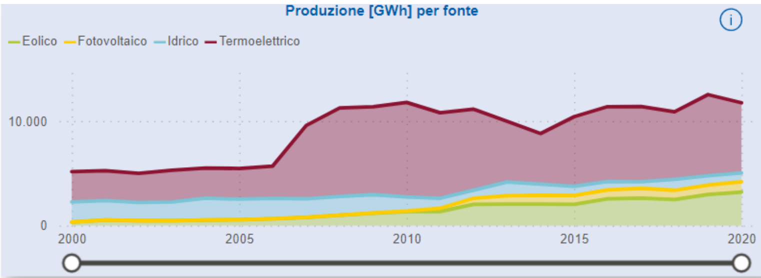

Figure 43 - Trend of energy production by source- time range: 2000-2020 (Source: TERNA S.p.A)

Table 12 - Energy production (GWh) by source for Campania and Caserta province. Years 2015 and 2019 (Source: TERNA S.p.A)

2015	wind	photovoltaic	hydroelectric	thermoelectric	Total
Campania	2028.6	848.7	871.3	6664.4	10413.0
Caserta	18.3	279.8	578.8	3906.7	4783.5
2019	wind	photovoltaic	hydroelectric	thermoelectric	Total
Campania	2964.1	907.0	892.2	7769.7	12533.0
Caserta	18.8	288.7	660.5	4504.2	5472.3

Since 2010 the production of energy by renewable sources has increased in Campania region (Figure 44): in 2019 in Campania region about 44% of total energy production was by renewable sources.
About the province of Caserta it is possible to observe an important increasing of bioenergy production while the increasing for the other sources is lower (Table 13)

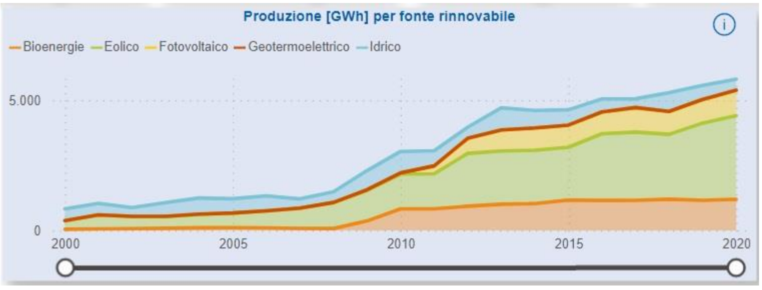

Figure 44 –Trend of energy production by renewable sources. Range time 2000-2020 (Source: TERNA S.p.A)

Table 13 - Energy production (GWh) by renewable sources for Campania region and Caserta province. Years 2015 and 2019 (Source: TERNA S.p.A)

2015	wind	photovoltaic	hydroelectric	thermoelectric (bioenergy)	Total
Campania	2028.6	848.7	587.9	1163.4	4628,6.0
Caserta	18.3	279.8	295.4	56.4	649,8
2019	wind	photovoltaic	hydroelectric	thermoelectric (bioenergy)	Total
Campania	2964.1	907.0	540.4	1155.5	5567.0
Caserta	18.8	288.7	308.7	73.5	689.8

The total consumption of energy during the considered five years remained generally the same:

2015	16545.9 GWh
2019	16601.7 GWh

Regarding Caserta province it is possible to highlight just a decreasing of consumption in the Agriculture sector with a simultaneous increasing for Industry sector (Table 14).

Table 14 - Energy consumption (GWh) for sector in Campania region and Caserta province. Years 2015 and 2019 (source: TERNA S.p.A)

2015	agriculture	household	industry	services
Campania	279.9	5484.1	4514.0	6267.8
Caserta	91.3	911.9	1060.7	1034.1
2019	agriculture	household	industry	services
Campania	279.2	5443.8	4660.8	6217.9
Caserta	76.81	924.2	1113.4	1041.5

4.4 Industry

According to the EUROSTAT data the contribution to Campania region GDP by Caserta is about 14.2%. In the following figures are reported the GDP per capita trend from 2015 to 2019. The values for Caserta are a little different from Campania region values.

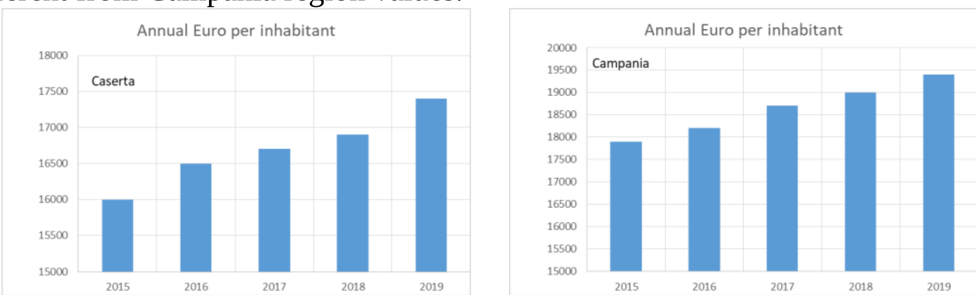

Figure 45 - GDP per capita (own elaboration from EUROSTAT data)

In the following figures regional and local gross value added (GVA) per sector are reported.

Figure 46 - Regional and local gross value added (GVA) per sector- Years 2015 and 2019 (own elaboration by Eurostat data)

Currently, the economic structure of the city is dominated substantially by trade and services without a consistent variation between 2015 and 2019, but it is based on a developed industrial apparatus, whose organic development started during the second half of 20th century. At that time the province of Caserta was called "Brianza of the South", referring to a well-developed industrial portion of the Lombardy region. This economic development was enhanced not only by a favorable geographic position but also by expertise and industriousness of his inhabitants that were useful after the economic crisis of 2008 too. In 2005 industrial export of the province of Caserta was around 750 million € and, except for 2014, from 2011 to 2017 always over 1 billion € (Izzo Francesco et al.) The secondary sector attracts substantial flows of commuters, who, together with the local population, find employment in the numerous construction companies, in large textile, chemical, food, construction materials, locomotives and railway-tram rolling stock factories, in mechanical workshops and metallurgical companies and in the many small and medium-sized businesses that exist.

About tertiary sector, the industry of tourism is driven by the visits to the Royal Palace (in 2021 Royal Palace was the fifth place more visited in Italy (Il Giornale dell'arte), but in the last years hotel accommodation capacity in Caserta has increased letting also a development of convention tourism (Italiapedia), as it evidenced in 2019 by an increment of employment in the sector that includes accommodation and food activities

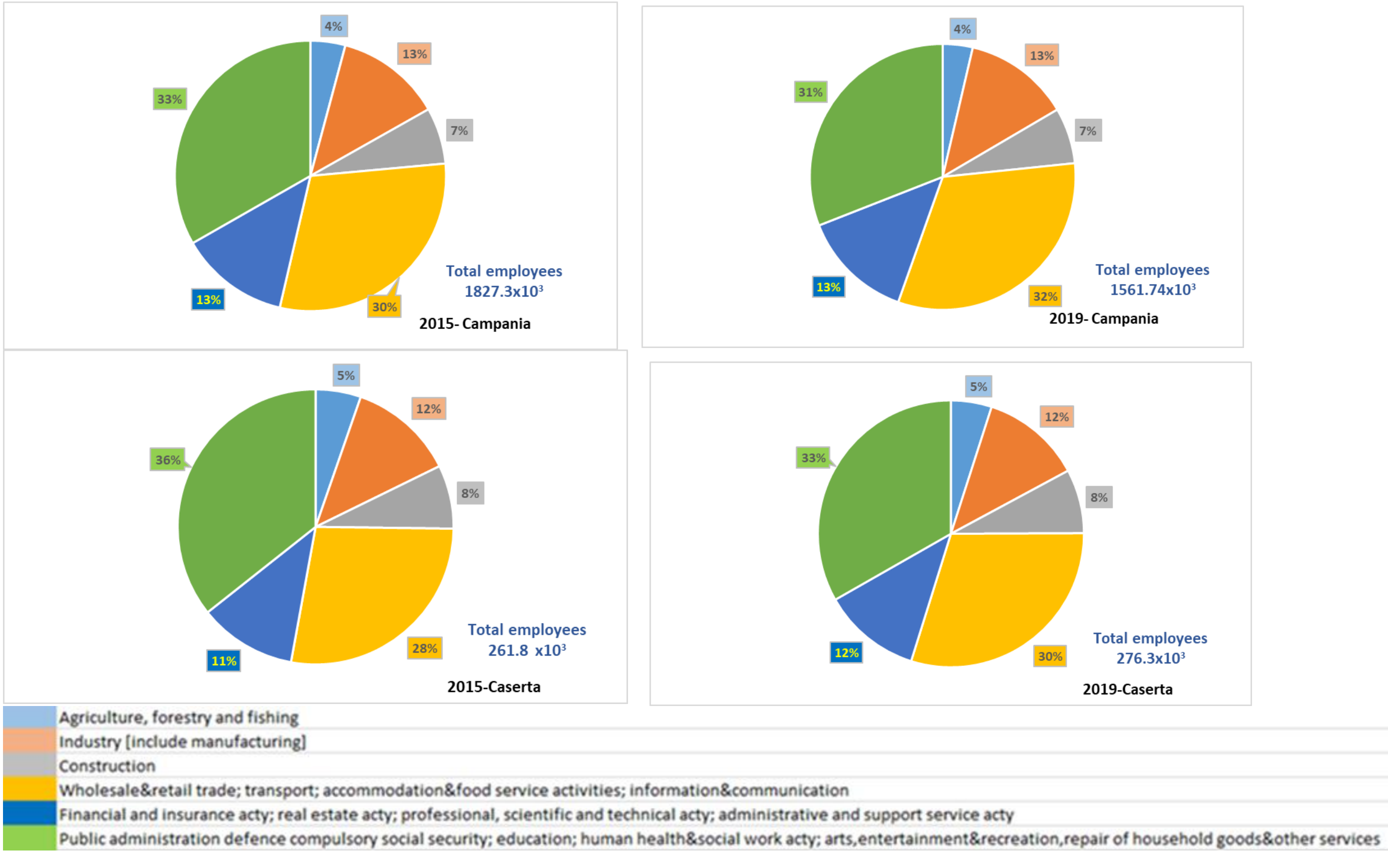

Figure 47 – Total employees per sector in Campania region and in Caserta. Years 2015 and 2019 (own elaboration from Eurostat data)

4.5 Transport and infrastructures

Local public transportation has just had a restyling with lines that cover the urban and external territory (Aircampania).
Several bus lines cover all the urban and extra urban territory, allowing the mobility of a consistent number of commuters that work in Caserta and its suburbs.

Connection with the rest of Region and Italy is assured by railway and motorway.
Caserta railway station is a hub for regional and national traffic, and represents an important interchange linking Rome and Naples to Bari. It is a stop for high speed trains (Trenitalia and Italo) between the North of Italy (Turin and Milan), South and Adriatic coast (Bari).

Figure 48 - High speed railway network (www.trenitalia.it)

Caserta is located in a strategic position with respect to the national and local motorway network: is the starting point of the A30 motorway to Salerno and is served by two exits of A1. This highway links the largest cities on the Tyrrhenian side of Italy: Milan, Bologna, Florence, Rome and Naples.

Figure 49 - Main Italian Highways (Wikipedia)

The nearest airport is Naples-Capodichino, located about 30 kilometers south.

In the next table the percentages of private vehicles per emission class and per fuel related to the years from 2015 to 2019 are reported. The trend towards vehicles with low emissions is still poor.

Table 15 - Urban mobility, private vehicles (own elaboration by ISTAT data)

	2015	2016	2017	2018	2019
Vehicles per emission class - %					
Euro 3 or lower	46.9	43.7	40.5	37.4	34.7
Euro 4	32.1	31	30.2	29.1	27.9
Euro 5	19	18	17.7	17.5	17.1
Euro 6	2	7.3	11.6	16	20.2
Euro 5/6 (diesel)	12.2	14.6	17	19.2	20.9
Total	100	100	100	100	100
Vehicles per fuel - %					
Petrol	46.8	46	45	44.1	43
Diesel	44.3	44.5	45.1	45.5	45.6
Low emissions	9	9.5	9.9	10.4	11.4
Total	100	100	100	100	100
Motocicles for emission class - %					
Euro 2 or lower	67.4	66.2	64.9	63.5	61.9
Euro 3	32.6	33.3	32.4	31.1	29.7
Euro 4 or upper	-	0.6	2.7	5.4	8.3
Total	100	100	100	100	100

4.6 Emission inventories

Spatially distributed emission data as used in EMEP models were downloaded by EMEP Centre on Emission Inventories and Projections (CEIP).
The resolution of grid emissions is 0.1°x0.1° long-lat.
Geographic coordinates of the Royal Palace in Caserta match to cell 14.35; 41.05 of the grid.
In this report were considered emissions into air of following main pollutants:
NO_x, SO_x, NH_3, NMVOC, CO and PM_{10}.
Sectors are defined as GNFR source category (UNECE 2015, Guidelines CE/EB.AIR/128.UNECE)
Aviation and shipping sectors are not considered because neither airport nor port are included in the concerned cell of the grid.
Public Power isn't considered because it isn't reported by Italian inventory.
The next tables 16 and 17 include total emission contribution in Mg/year per sector.
Figures 50 and 51 report the contribution of each pollutant for each sector in percentage to the total annual emissions.

Table 16 – Sector contribution (Mg) to the annual total emissions for Caserta. Year 2015
(Data source: EMEP/CEIP 2021)

Year 2015	NOx	SOx	NH3	NMVOC	CO	PM10	Total
	Mg	Mg	Mg	Mg	Mg	Mg	Mg
Industry	2362.31						**2362.31**
OtherStationaryComb	196.16	16.45	2.17	161.14	1314.84	90.48	**1781.24**
Fugitive			13.40	151.91		1.68	**167.00**
Solvents	0.47	0.05	1.08	1021.77	14.45	8.16	**1045.99**
RoadTransport	660.41	0.62	8.41	242.70	972.86	39.47	**1924.48**
Offroad	54.19	0.43	0.02	14.15	98.79	4.70	**172.28**
Waste	3.99	0.39	26.87	30.98	161.10	9.87	**233.19**
AgriLivestock			6.79	20.03		0.56	**27.38**
AgriOthe			28.52	4.50		3.17	**36.18**
Total	**3277.54**	**17.94**	**87.25**	**1647.18**	**2562.04**	**158.10**	**7750.05**

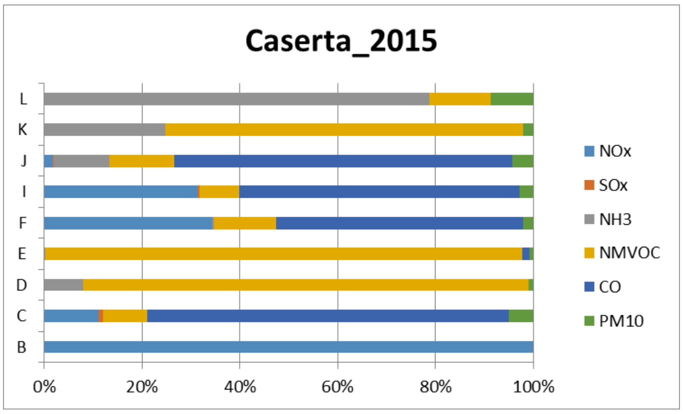

L	AgriOthe
K	AgriLivestock
J	Waste
I	Offroad
F	RoadTransport
E	Solvents
D	Fugitive
C	OtherStationaryComb
B	Industry

Figure 50 - Sector contribution (%) to the annual total emissions for Caserta. Year 2015
(Data source: EMEP/CEIP 2021)

Table 17 – Sector contribution (Mg) to the annual total emissions for Caserta. Year 2019 (Data source: EMEP/CEIP 2021)

Year 2019	NOx	SOx	NH3	NMVOC	CO	PM10	Total
	Mg	Mg	Mg	Mg	Mg	Mg	Mg
Industry	2037.25						**2037.25**
OtherStationaryComb	193.24	15.86	1.75	147.71	1193.15	79.63	**1631.34**
Fugitive			9.54	127.85			**137.39**
Solvents	0.43	0.04	0.98	1159.08	13.14	6.99	**1180.66**
RoadTransport	507.59	0.63	7.62	195.34	787.71	31.76	**1530.66**
Offroad	40.06	0.43	0.01	9.75	87.30	2.79	**140.35**
Waste	0.69	0.25	26.51	22.47	20.96	6.33	**77.20**
AgriLivestock			6.57	20.60		0.56	**27.73**
AgriOthe			28.43	4.43		3.20	**36.06**
Total	**2779.26**	**17.22**	**81.40**	**1687.22**	**2102.26**	**131.26**	**6798.62**

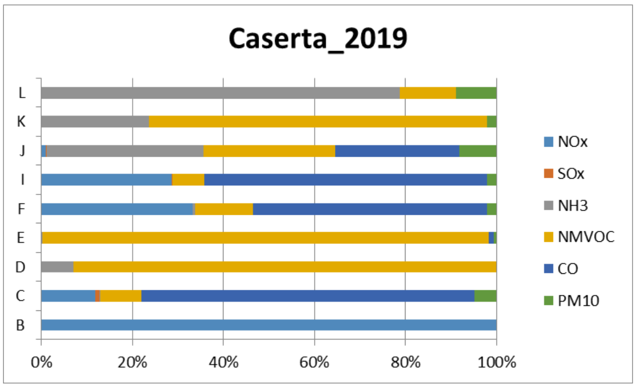

L	AgriOthe
K	AgriLivestock
J	Waste
I	Offroad
F	RoadTransport
E	Solvents
D	Fugitive
C	OtherStationaryComb
B	Industry

Figure 51 - Sector contribution (%) to the annual total emissions for Caserta. Year 2019 (Data source: EMEP/CEIP 2021)

In terms of sectors the highest contribution is ascribed to Industry followed by Other Stationary Combustion, Road Transport and Solvents as expected on the basis of economic trend in Caserta dominated by trade and service sectors, but with an industrial vocation.
Industry appears to hold the majority of CO and NOx emissions, followed by the Road Transport sector.
All sectors show a decreasing trend into the concerned temporal range except the sector connected to the Agricultural activities and Solvents sector that remain substantially constant.

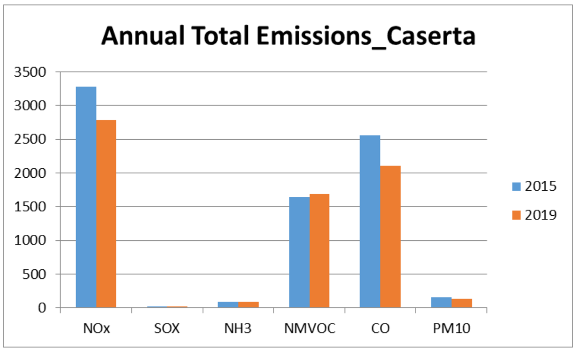

Figure 52 - Annual total emissions of main pollutants into air in Caserta. Comparison 2015 and 2019 (Data source: EMEP/CEIP 2021)

In Figure 52 the contribution of each pollutant to the total annual emission is reported as a comparison

between years 2015 and 2019.
NO_x, PM_{10} and CO emissions show a decreasing trend while the other ones show nearly constant values or a light increase (NMVOC).

4.7 Air Quality - Ground level air pollutants

Air pollutants monitoring stations	
Caserta_CE51 urban background	41.07869; 14.33838
Caserta_CE52 urban traffic	41.07693; 14.3312

Figure 53 – Position of air pollutants monitoring stations[9]

The air pollutants data in Caserta were downloaded by official site ARPA Campania collected by the local network of monitoring stations (Figure 53): CE51 as urban background and CE52 as urban traffic station.
Unfortunately SO_2 concentration data are not measured by these two monitoring stations. SO_2 concentration data were downloaded by EMEP MSC-W model.
Ozone concentration data measured by CE51 station can be considered valid for CE52 monitoring station too.

Figure 54 reports trends of the annual mean of the main pollutants measured at the monitoring station for investigated temporal range: 2015-2019.
To appreciate the trend over the past, the data for the two stations concentration are reported after removing Ozone concentration values too.

[9] Google Earth Pro-Image Landsat/Copernicus

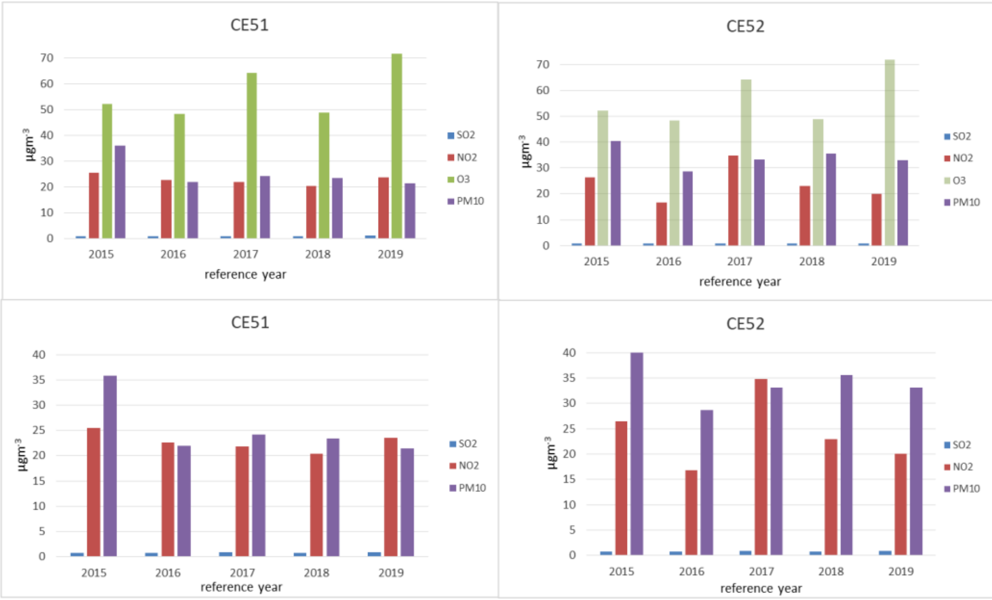

Figure 54 – Air pollutants data by monitoring stations CE51 and CE52. Time range: 2015-2019

Even if CE52 station is closer to the Royal Palace than CE51 station, the latter one better describes the surroundings of the UNESCO monument. In fact the location of the Royal Palace is far from the street and in a garden surrounded by trees.
NO_x concentration trend doesn't appear linear along the time for both monitoring stations. It could be appreciate a decreasing trend for data measured at urban traffic station from 2017. Data measured at background station are substantially unchanged along the time, highlighting that all measures adopted to reduce NO_x emissions don't have effect on low traffic area.
PM_{10} concentration trend shows the same trend of NO_x for both monitoring stations.
As expected concentrations of SO_2 have dropped significantly and now does not represent an important air polluting compound: SO_2 concentrations are low and constant along the time.

4.8 Implications on the UNESCO Cultural Heritage Site: The Royal Palace

Figure 55 - The main façade of the Royal Palace of Caserta[10]

The Royal Palace of Caserta in 2021 was among the five most visited places in Italy (il Giornale dell'arte The monumental complex at Caserta, located about 20 miles north of Naples, was designed in the second half of the 18th century by the architect Luigi Vanvitelli according to the wishes of the Bourbon king Charles III, as soon as he became king of Naples, to rival Versailles and the Royal Palace in Madrid and to display the power and grandeur of the new kingdom, no longer a part of the Spanish reign. It includes the Royal Palace (Reggia in Italian) with a park, gardens and wooded area, as well as the Aqueduct Carolino and the industrial complex of San Leucio, built for the production of silk. The complex is considered the last major architectural work in the Italian Baroque style and is the largest royal residence in the world. The complex was listed as a UNESCO World Heritage Site in 1997 (18th-Century Royal Palace at Caserta with the Park, the Aqueduct of Vanvitelli, and the San Leucio Complex). The property (N 41° 4' 23.988" E 14° 19' 35.004") extends for 87.37 ha and its buffer zone is 110.76 ha. The number of visitors to Caserta's attractions is around 0.7 million a year.
The Royal Palace is located on a central axis which connects and unifies the entire complex. Along the central axis, wide lawns, flowerbeds, ponds and fountains, decorated with large sculptural groups and other architectural elements, are present. Just behind the Reggia itself lies a landscaped park, a typical example of an Italian garden. This perspective terminates in the scenic backdrop of the Great Waterfall (Grande Cascata), where water cascades down from a height of 150 m into an ornate basin that depicts the Roman goddess Diana bathing while observed by Actaeon. Water needed to keep the water games, the Royal Palace, the silk factory and surrounding communities was brought from spring over a distance of 38 km through the new built structure called the Acquedotto Carolino.
The Royal Palace is the primary feature of the UNESCO site. The palace has a rectangular plan, measuring 247 x 190 m, and a surface of approximately 47,000 m^2. It is 38 meters high and has five floors

[10] Photo by Mr.TinMD Creative Commons

in addition to the underground level housing the kitchens, cellars and workshops. Of all the royal palaces in the world, Caserta is by far the largest in terms of volume, with more than 2 million m^3. The four sides are connected by two buildings intersecting at right angles, forming four inner courtyards which are also rectangular (each of 3,800 m^2). The structural units, intersected at right angles to one another, have their apexes extended a little beyond the perimeter line, giving rise to articulations accentuated by the pilasters of these elongated apexes. In front of the main façade is the elliptical parade ground. An imposing portico constitutes the ideal connection with the park and the waterfall, scenographically placed at the peak of the vanishing point thus created.
The immense residence contains 1200 rooms including 24 state apartments, a monumental white marble staircase (18.50 meters wide, 14.50 meters high and 117 steps) giving access to the royal apartments, 34 staircases, 1742 windows (245 windows on the main façade and the same on the back), a magnificent library, a chapel (the Palatine Chapel, inspired by a chapel of the same name at Versailles) and the Royal Theatre, a smaller version of the Teatro San Carlo opera house in Naples.
The interior of the palace is decorated with frescoes, stuccoes, sculptures, bas-reliefs and inlaid floors.
The masonry of the building is in squared blocks of yellow tufa stone placed in place with mortar, with a thickness of 3.50 m on the ground floor. On the outside, the first two floors are covered with travertine slabs (Pietra di Bellona) while the upper floors are faced with clay bricks. Some parts of the external surface is coated with plaster (based on lime and pozzolana with a stucco finish based on lime and stone or marble powder) colored or painted to simulate a fake brick curtain. The exterior of the palace is adorned with half columns, fluted pilasters, embossed architectural elements (cornices, window frames, capitals, sculptural friezes) in Pietra di Bellona or white Carrara marble and with architectural elements, subordinate to the main elements, in painted plaster. The main façade has three vaulted entrances and 2 doorways. The façade giving onto the park is similar, but even more ornate, with fluted pilaster framed windows. The whole structure is crowned by a penthouse punctuated by small windows and shaded by a frame surmounted by a balustrade in white Carrara marble and Pietra di Bellona. The roof is formed with large tiles and channels, as well as the bricks for the floors.
The materials needed in the construction of the work were drawn largely from existing quarries in the area or in the territories of the kingdom: San Nicola la Strada (tufa), Bellona (travertine), Mondragone (gray marble), San Leucio (lime), Bacoli (pozzolan), Gaeta (arena), Capua (bricks and the like), Sicily, Calabria and Puglia for different marbles. For the statues and some moldings, the white Carrara marble was used.
Since the 1990s, funding problems have led to serious shortcomings in the building's maintenance, culminating in the autumn of 2012 in the collapse of two structures, the terminal cornice of the main façade and the gable of a window, highlighting the state of decay of the architectural decorations. It was determined that the falling of the larger stone blocks was caused by the rusting of the ancient iron anchoring grips due to the infiltration of water and favored by the growth of weeds in the cracks. An extensive restoration project was then launched.
The restoration work was preceded by instrumental investigations (using modern technologies like laser scanning, ground-penetrating radar, pulse induction and thermal imaging) and close inspections aimed at analyzing in detail the type of material, its state of conservation, the presence of any anomalies and at mapping of the disconnections of the stone material. The façades of the monumental complex were checked and repaired. The stone parts of the façade were cleaned with ammonium carbonate, freed from the so-called "black crusts" caused by pollution and from mosses, lichens and plants, and reinforced with injections of hydraulic mortar. The original metal cramps were replaced by small fiberglass pins and bars of stainless steel.
The restoration work on the external and internal facades for a total surface area of 74,000 square meters, lasted two and a half years and had a full cost of €15 million, in part co-financed by the European Regional Development Fund (ERDF**).**

Being located in the heart of the city, the Royal palace is subject to the environmental pressure caused by air pollution from the town, but at same time it could be protected by surrounding trees**.**

Nitric acid is not measured by the Caserta Air Quality Monitoring Network, so atmospheric nitric acid concentrations were calculated from NO_2, O_3, relative humidity (Rh) and temperature (T) by using the following empirical function derived within the MULTI-ASSESS project (MULTI-ASSESS, 2005):

$$\mathbf{HNO_3 = 516 \times e^{-3400/(T+273)} ([NO_2] \times [O_3] \times Rh)^{0.5}}$$

where

[HNO_3] = annual average concentration, $\mu g\ m^{-3}$
[NO_2] = concentration, $\mu g\ m^{-3}$ - annual
average [O_3] = concentration, $\mu g\ m^{-3}$ - annual
average T = temperature, °C – annual average
Rh = relative humidity, % - annual average

The methodology used for the estimation of the damage due to attack of atmospheric pollutants at the selected UNESCO cultural heritage sites is based on the use of the dose-response functions, first year exposure, for the multi-pollutant situation:

$$\mathbf{R = 4.0 + 0.0059[SO_2]Rh_{60} + 0.054Rain[H^+] + 0.078[HNO_3]Rh_{60} + 0.0258PM_{10}}$$

where

R= surface recession, µm
Rh_{60}= Rh – 60 when Rh > 60, 0 otherwise (Rh = relative humidity, % - annual average)
Rain= amount of precipitation, mm $year^{-1}$ - annual average
[SO_2]= concentration, $\mu g\ m^{-3}$ - annual average
[H^+]= concentration, mg l^{-1} - annual average
[HNO_3]= annual average concentration, $\mu g\ m^{-3}$
PM_{10}= annual average concentration, $\mu g\ m^{-3}$

The multi-pollutant dose-response function relate damage to limestone, expressed in terms of rate of surface corrosion, to a range of atmospheric pollutants: sulphur dioxide (SO_2), nitric acid (HNO_3), total acidity of rainfall (H^+), and particulate matter (PM_{10}). Environmental parameters also play a role, as reflected by the presence in the dose-response function of the two terms amount of precipitation (Rain) and relative humidity (Rh).

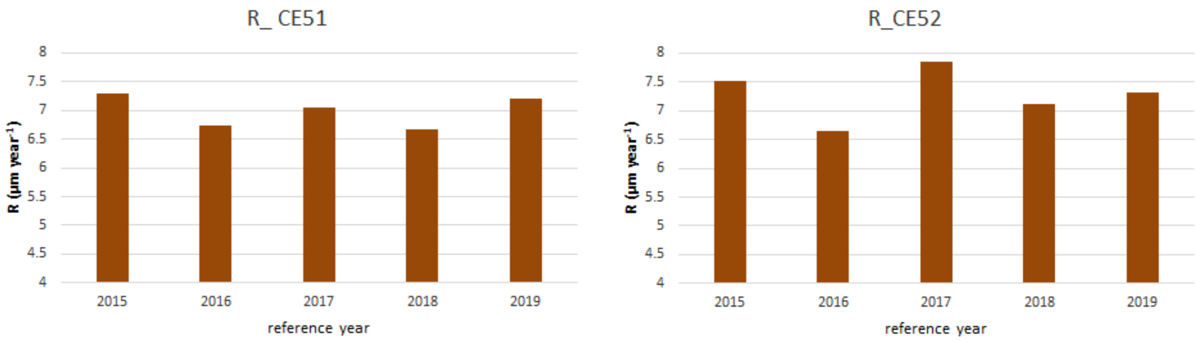

Figure 56 – Surface recession, $\mu m year^{-1}$

As expected surface recession trend follows the same shape of pollutants concentrations: not linear trend. In addition the value of Ozone concentration recorded in 2019 higher than in the previous years, influences the value of surface recession producing a light increase of R.

Predicted soiling rate of limestone in Caserta was calculated by applying the dose-response function:

$$\Delta R/Ro = 1 - \exp(-PM_{10} \times t \times K)$$

Where
$\Delta R/Ro$ = relative loss of reflectance,
PM_{10} = concentration of PM_{10} ($\mu g\ m^{-3}$),
t = time (days)
K = soiling constant.

For limestone a soiling constant of 6.5×10^{-6} could be used, but it isn't officially accepted because of its high variability. So to be conservative the same calculation has been made using the lowest soiling constant reported on Mapping Manual, 3.47×10^{-6} for Polycarbonate Membrane material. In this way it is possible to assert with a good approximation that the value of **Δ**R/Ro is within the calculated range.
This dose-response function was used to predict the years to reach 30% of loss in reflectance as a function of the ambient PM_{10} concentrations to which the material is exposed.
30% of loss in reflectance is the "tolerable soiling before action", which represents the threshold triggering significant adverse public reaction of what constitutes acceptable soiling (Mapping Manual Ch.4).
In the following figures the number of years for reaching 30% of loss in reflectance on the basis of PM_{10} measured by the two monitoring stations in Caserta is reported.

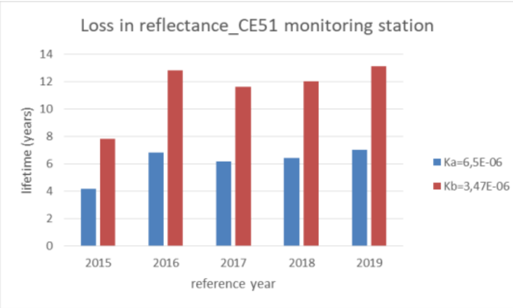

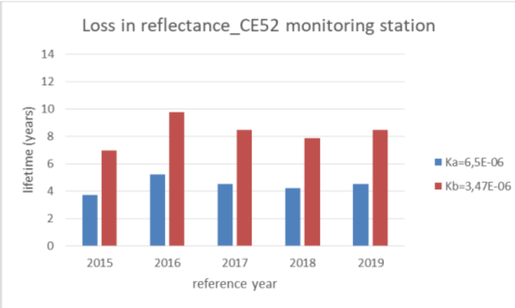

Figure 57 – Estimated lifetime of limestone for soiling (30% loss in reflectance)

For cultural heritage objects a period of 10-15 years is considered to be appropriate.
The 2050 target of 15 years isn't reached, even with the lowest constant.

4.9 References

Aircampania https://aircampania.it/

Beni culturali Reggia di Caserta https://reggiadicaserta.cultura.gov.it/

Climate- data https://it.climate-data.org/

EMEP Centre on Emission Inventories and Projections (CEIP) https://www.ceip.at/the-emep-grid/gridded-emissions

Il Giornale dell'Arte , april 2022 https://www.ilgiornaledellarte.com/articoli/la-classifica-mondiale-dei-musei-pi-visitati/138962.html

ISTAT Istituto nazionale di Statistica https://demo.istat.it/

Italiapedia www.italiapedia.it

Izzo Francesco et al. "Economia a Caserta Performance delle imprese industriali e attrattività del territorio" Economy Department, Vanvitelli University, Caserta,2018 https://www.economia.unicampania.it/images/Ricerca/working_paper/caserta_economia_018_copia.pdf

Mapping manual Ch.4 https://www.umweltbundesamt.de/en/document/mapping-manual-ch-4

MULTI-ASSESS, 2005. MULTI-ASSESS. Model for multi-pollutant impact and assessment of threshold levels for cultural heritage. Final report. http://www.corr-institute.se/MULTI-ASSESS/

TERNA S.p.A. https://www.terna.it/it/sistema-elettrico/statistiche/pubblicazioni-statistiche

UNECE 2015, Guidelines for Reporting Emissions and Projections Data under the Convention on Long-range Transboundary Air Pollution. ECE/EB.AIR/128.

5 Discussion

Because each monument is not an isolated entity, this report concerns the study of the relationship between the environmental context surrounding some selected UNESCO sites and the air pollution responsible for the corrosion and soiling effects of the material. Three UNESCO sites located in three cities with different climatic, topographic and emission-related characteristics were chosen on the basis of maintenance cost due to air pollution (assessed in the report No.86): Saint Domnius, Split in Croatia, Würzburg Residence, Bavaria, Germany and Royal Palace, Caserta, Italy.

	Limestone (corrosion)	Limestone (soiling)
St. Domnius Cathedral	Low	Medium
Würzburg Residence	Medium	Medium
Royal Palace of Caserta	Very High	High/Very High

Figure 58 – Investigated UNESCO sites

To assess the damage due to attack of atmospheric pollutants at the selected UNESCO world cultural heritage sites, the methodology based on the use of dose-response function was used to estimate limestone surface recession and soiling.
Temporal range investigated is five years from 2015 to 2019.
Air pollutants concentrations were downloaded from public sites reporting data measured at local monitoring stations.
Meteorological data were averaged over the five-year interval studied to highlight the effect of pollutants.
Emissions data were downloaded from EMEP Centre on Emission Inventories and Projections (CEIP).

In a multi-pollutant scenario, nitric acid (produced from atmospheric nitric oxides) and particulate matter seem to play a prominent role in determining damage of limestone. Nitric acid and particulate matter concentrations are higher in cities, where most of our cultural heritage is situated. The acidity of precipitation, expressed by the pH value, seems to have a little impact on corrosion in the current situation. PM_{10} dominates for soiling of materials.
Road traffic is an important source for nitric oxides and particular matter not only for direct combustion emissions but also for non-exhaust sources like as tyre-wear, break-lining, road abrasion, etc. together with re-suspension of deposited dust on the surface.
Although road transport is the main emission source in urban areas, further emission reductions should be considered for the other sources. In some cases, the weights of industry and service activities play important roles in air quality levels.
In addition to the local origin, the levels of pollutants, with a negative impact on materials used in objects of cultural heritage, are significantly affected by sources outside the city or even outside the country. High PM_{10} concentrations may be due to natural sources as sea spray or intrusion of Saharan dust especially in the South of Europe.

Inside the main residential areas, incomplete biomass combustion for heat production, e.g. in domestic boilers, wood stoves and fireplaces can be an important PM_{10} emission source on specific months during winter contributing to increase the risk of deterioration of the studied monuments made of marble/limestone.

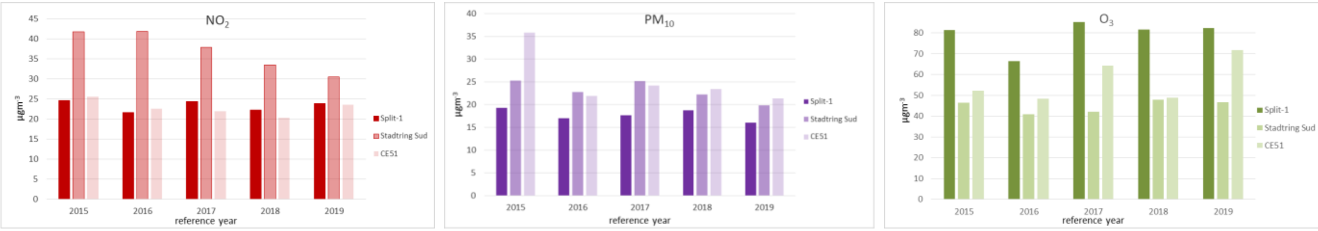

Figure 59 – Summary of air pollutants concentration for the investigated three sites

Within investigated temporal range it is observed a light decrease of NO_2 and PM_{10} concentrations in all cities that host UNESCO sites

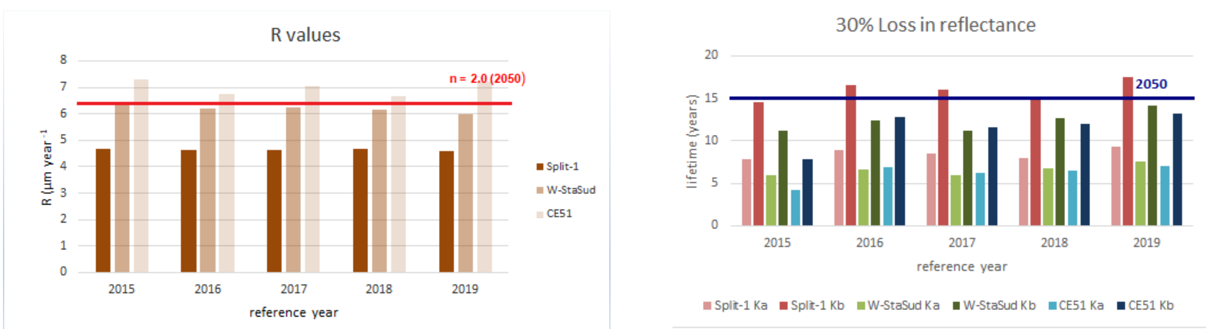

Figure 60 – Summary of surface recession and 30% loss in reflectance for the investigated three sites

Figure 60 shows limestone recession rate, first year of exposure, as micrometer per year and limestone soiling as years for 30% loss in reflectance. It isn't observed a real trend, more or less the values remain the same.
The decrease of pollutants concentrations are enough to have R values generally close to the target for the year 2050 (6.4 µm $year^{-1}$) except for Caserta.
The 2050 target of 15 years before action is reached just for Split only considering the lowest value for soiling constant. Using not official accepted constant for limestone, number of years to reach 30% loss of reflectance increases but remains far from 2050 target.
St Domnius Cathedral in Split is located very close to the port and is affected by port activity emissions. An analysis by transport & Environment that mentions Split among others cities highlights PM emissions from shipping are connected to the quality of fuel used, consequently even a relatively small number of cruise ships can emit a large amount of air pollution (Faig Abbasov, Thomas Earl, Nicolas Jeanne, Bill Hemmings, Lucy Gilliam, and Carlos Calvo Ambel "One Corporation to Pollute Them All. Luxury cruise air emissions in Europe" In house analysis by Transport & Environment, June 2019).
Apparently Würzburg and Caserta are comparable both in terms of pollutants concentration and in the position of UNESCO monuments, however the limestone recession rate values are different. R calculation is affected by concentration of HNO_3, linked to O_3 concentration, and meteorological data, with temperature and rain amount higher in Caserta. It would be a mistake to attribute the difference in the value of R mainly to the weather data: even if Caserta has about half the inhabitants of Würzburg, traffic emissions are comparable and industrial emissions are far greater for Caserta.

To reduce the risks that threaten our cultural heritage and consequently the economic cost of maintenance of cultural heritage buildings further mitigation actions need to apply an efficient control on emission sources.
Road transport is a very important source of poor air quality in the cities. Because of the investigated

UNESCO monuments are located in metropolitan areas it would be good to implement traffic reduction policies in busy areas increasing public transport and encouraging the use of low-emission vehicles and car sharing.
In addition a further powerful improvement for research activities to study and realize systems for abatement of industrial emissions is necessary.
Regarding the reduction of shipping emissions, good news for the Mediterranean area comes from International Maritime Organization (IMO). As is known, from 1st January 2020 the sulfur content limit in world maritime waters was raised to the maximum value of 0.5% mass by mass from the previous 3.5% m/m on the basis of agreement known as “IMO 2020”. A stricter limit of 0.10% m/m established by IMO already exists in emission control areas (ECAS): the Baltic Sea area; the North Sea area; the North American area (covering designated coastal areas off the United States and Canada); and the United States Caribbean Sea area (around Puerto Rico and the United States Virgin Islands).
“In 2022, MEPC 78 agreed to designate the entire Mediterranean Sea as an emission control area, meaning that ships will - from 2025 - have to comply with more stringent controls on sulphur oxide emissions. The Committee approved proposed amendments to MARPOL Annex VI, with a view to adoption at MEPC 79, which will designate the Mediterranean Sea, as a whole, as an Emission Control Area for Sulphur Oxides (SOx-ECA) and particulate matter. The amendment could enter into force in mid-2024, with the new limit taking effect from 2025.” (https://www.imo.org/en/MediaCentre/HotTopics/Pages/Sulphur-2020.aspx).

6 Acknowledgements

The authors wish to acknowledge present and former members of Task Force, especially those responsible for assessments and contacts at the UNESCO sites, for the useful discussion and comments.
A special thanks to Ilaria D’Elia.